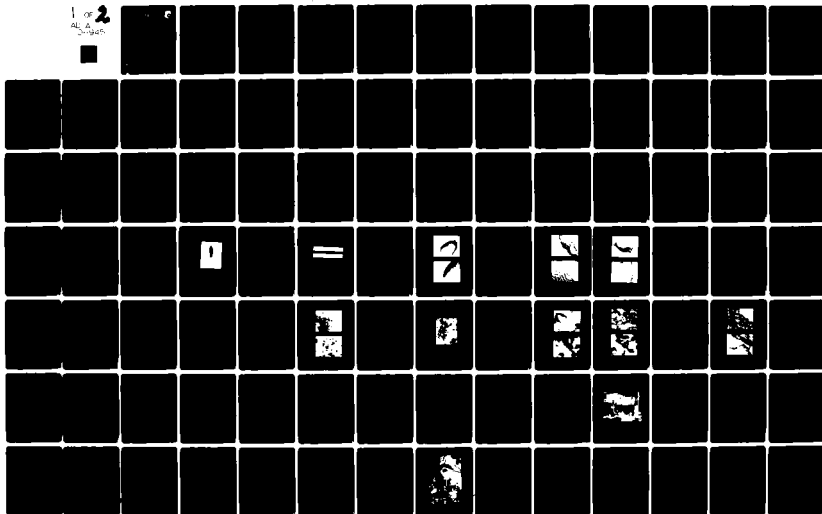


AIRSEARCH MFG CO OF ARIZONA PHOENIX F/G 21/4
COMPOUND CYCLE TURBOFAN ENGINE (CCTE). TASK IX. CARBON-SLURRY F--ETC(U)
MAR 80 T W BRUCE, H MONGIA F33657-77-C-0391
21-3365-A AFWAL-TR-80-2035 NL

AFWAL-TR-80-2035

NL

1 of 2



AD A089451

LEVEL II

AFWAL-TR-80-2035



6
COMPOUND CYCLE TURBOFAN ENGINE
(CCTE).
TASK IX.

Carbon-Slurry Fuel Combustion
Evaluation Program

2

14 21-3365-A

10
I. W. BRUCE
H. MONGIA

AIRSEARCH MANUFACTURING COMPANY OF ARIZONA

A Division of the Garrett Corporation

P.O. Box 5217 Phoenix, Arizona 85010

11
MARCH 1980

TECHNICAL REPORT AFWAL-TR-80-2035

Final Report for Task IX for Period June 1978 - September 1978

Prepared for
DEFENSE ADVANCED RESEARCH PROJECTS AGENCY
1400 Wilson Boulevard, Arlington, Virginia 22209
Contract No. F33657-77-C-0391

15
AERO PROPULSION LABORATORY
AIR FORCE WRIGHT AERONAUTICAL LABORATORIES
AIR FORCE SYSTEMS COMMAND
WRIGHT-PATTERSON AIR FORCE BASE, OHIO 45433

DTIC
ELECTE
S SEP 12 1980 D
E

JOE

404746

80 9

8


015


NOTICE

When Government drawings, specifications, or other data are used for any purpose other than in connection with a definitely related Government procurement operation, the United States Government thereby incurs no responsibility nor any obligation whatsoever; and the fact that the government may have formulated, furnished, or in any way supplied the said drawings, specifications, or other data, is not to be regarded by implication or otherwise as in any manner licensing the holder or any other person or corporation, or conveying any rights or permission to manufacture use, or sell any patented invention that may in any way be related thereto.

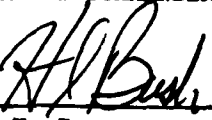
This report has been reviewed by the Office of Public Affairs (ASD/PA) and is releasable to the National Technical Information Service (NTIS). At NTIS, it will be available to the general public, including foreign nations.

This technical report has been reviewed and is approved for publication.


ROGER L. SPENCER
Project Engineer


JACK RICHENS
Chief, Performance Branch

FOR THE COMMANDER


H. I. BUSH
Deputy Director
Turbine Engine Division

"If your address has changed, if you wish to be removed from our mailing list, or if the addressee is no longer employed by your organization please notify AFWAL/POTA, W-PAFB, OH 45433 to help us maintain a current mailing list".

Copies of this report should not be returned unless return is required by security considerations, contractual obligations, or notice on a specific document.

SECURITY CLASSIFICATION OF THIS PAGE (When Data Entered)

REPORT DOCUMENTATION PAGE		READ INSTRUCTIONS BEFORE COMPLETING FORM
1. REPORT NUMBER AFWAL-TR-80-20351	2. GOVT ACCESSION NO. AD-A089451	3. RECIPIENT'S CATALOG NUMBER
4. TITLE (and Subtitle) CCTE-TASK IV Carbon-Slurry Fuel Combustion Evaluation Program		5. TYPE OF REPORT & PERIOD COVERED Final Report
7. AUTHOR(s) T. W. Bruce H. Mongia		6. PERFORMING ORG. REPORT NUMBER 21-3365-A
8. PERFORMING ORGANIZATION NAME AND ADDRESS AiResearch Mfg. Co. of Arizona P.O. Box 5217, Phoenix, Az. 85010		9. CONTRACT OR GRANT NUMBER(s) F-33657-77-C-0391
11. CONTROLLING OFFICE NAME AND ADDRESS Advanced Research Projects Agency 1400 Wilson Boulevard Arlington, Va. 22209		10. PROGRAM ELEMENT, PROJECT, TASK AREA & WORK UNIT NUMBERS Project 62301E Task ABPA002
14. MONITORING AGENCY NAME & ADDRESS (if different from Controlling Office) Aeronautical Systems Division (YZ/KC) Wright-Patterson AFB, Ohio 45433		12. REPORT DATE March 1980
		13. NUMBER OF PAGES 92
		15. SECURITY CLASS. (of this report) Unclassified
		16. DECLASSIFICATION/DOWNGRADING SCHEDULE
16. DISTRIBUTION STATEMENT (of this Report) Approved for public release; distribution unlimited.		
17. DISTRIBUTION STATEMENT (of the abstract entered in Block 20, if different from Report)		
18. SUPPLEMENTARY NOTES		
19. KEY WORDS (Continue on reverse side if necessary and identify by block number) Carbon-Slurry Fuel High Efficiency Heat Engine Combustion Compound Cycle Direct Injection Cruise-Missile		
20. ABSTRACT (Continue on reverse side if necessary and identify by block number) The carbon-slurry fuel evaluation program demonstrated the feasibility of running a currently available carbon-slurry fuel in a combustion rig and a turbine engine. This program also established the preliminary design criteria for operating on carbon-slurry fuels. Subcontracts work was performed by Pennsylvania State for fuel droplet measurements and by Suntech, Inc. for fuel development and manufacture.		

PREFACE

This report is submitted by the AiResearch Manufacturing Company of Arizona, a division of The Garrett Corporation, in accordance with the requirements of Contract F33657-77-C-0391 (CRDL Sequence No. 1), and represents the final technical report for the Carbon-Slurry Fuel Combustion Evaluation Program. This program was conducted as an add-on to the Compound Cycle Turbofan Engine Program (Contract F33657-77-C-0391). AiResearch acknowledges the direction and assistance rendered by Mr. Roger Spencer of AFAPL who is the Project Manager for the Compound Cycle Turbofan Engine Program, and Mr. James McCoy and Dr. Alvin Bopp of the Air Force Fuels and Lubrication Branch who were technical monitors for the carbon-slurry fuel effort.

Accession For	
NTIS GRA&I	<input checked="checked" type="checkbox"/>
DDC TAB	<input type="checkbox"/>
Unannounced	<input type="checkbox"/>
Justification	
By _____	
Distribution/	
Availability Codes	
Dist.	Avail and/or special
A	

TABLE OF CONTENTS

	<u>Page</u>
I INTRODUCTION	1
II SUMMARY AND CONCLUSIONS	4
III TECHNICAL DISCUSSION	8
1. Fuel Development	8
a. Fuel Development Background	8
b. Slurry Formulation, Preparation, and Characterization	8
(1) Slurry Formulation	9
(2) Slurry Preparation	10
(3) Slurry Characterization	10
(4) Slurries Submitted for Burning Tests	11
c. Slurry Development Program	11
(1) Formulations with Varied Additive Package Components	16
(2) The Use of the Brookfield Viscometer to Characterize Slurries	16
d. Results of Components of the Additive Packages on Rheological Properties of Slurries	19
2. Fuel Droplet Measurements	24
a. Fuel Droplet Measurement Background	24
b. Fuel Droplet Experimental Program Description	29
(1) Apparatus	29
(2) Instrumentation	31
(3) Test Conditions	33
c. Fuel Droplet Experimental Results	36
(1) Droplet Processes in Air	36
(2) Droplet Processes in a Turbulent Flame	45
d. Conclusions	65
3. Combustion Evaluation of Slurry-Fuel Samples	67
a. Combustion Evaluation Background	67
b. Atmospheric Testing	68
c. ETJ131 Combustor Pressure Rig Testing	80
d. ETJ131 Demonstrator Engine Testing	88

LIST OF ILLUSTRATIONS

<u>Figure</u>	<u>Title</u>	<u>Page</u>
1	Flow Diagram for Full-Scale Combustion System Development for Operation of Carbon-Slurry Fuel	2
2	Shear Rate Versus Shear Stress for Sample of 50 Percent by Weight of MT Black in JP-10	14
3	Viscosity-Temperature Chart for Sample 790-928 (50 Percent by Weight of MT Black in JP-10)	15
4	Torque and Speed Relationships for Determining Brookfield Viscosity	18
5	Fluidity as a Function of Percent MT Black	21
6	Yield Point as a Function Additive Concentration (50-Percent Black in JP-10)	22
7	Component A on MT Black in JP-10 Effect of Concentration on Torque/RPM Slope (50-Percent Black in JP-10)	23
8	Effect of Additive Composition and Concentration of Deflocculation of MT Black in JP-10	25
9	Test Apparatus Schematic	30
10	Photograph of the Turbulent Gas Diffusion Flame	35
11	Dark Field Motion Picture Photographs of a Catalyzed Slurry Droplet Burning in Air	37
12	SEM Photograph of Residue Following the Evaporation of a Catalyzed Slurry Drop in Air (Top x 50, Bottom x 200)	39
13	SEM Photograph of Residue Following the Combustion of a Noncatalyzed Slurry Drop in Air (Top x 50, Bottom x 400)	41
14	SEM Photograph of Residue Following the Combustion of a Catalyzed Slurry Drop in Air (Top x 100, Bottom x 400)	42
15	Droplet Diameter as a Function of Time for Three Fuels Burning in Air	43

LIST OF ILLUSTRATIONS

<u>Figure</u>	<u>Title</u>	<u>Page</u>
16	Flow Properties and Slurry Droplet Combustion Regions in the Turbulent Flame	46
17	SEM Photograph of Residue from a Catalyzed Slurry Drop in the Fragmentation Region, $x/d = 75$ (Top x 150, Bottom x 5000)	51
18	SEM Photograph of the Residue from a Catalyzed Slurry Drop in the Noncombusting Region, $x/d = 149$ (x 5000)	53
19	SEM Photographs of Residue from a Catalyzed Slurry Drop in the Full Combustion Region, $x/d = 340$ (Top x 100, Bottom x 5000)	55
20	SEM Photographs of Residue from a Catalyzed Slurry Drop in the Glowing Region, $x/d = 489$ (Top x 2000, Bottom x 5000)	56
21	SEM Photographs of Residue from a Catalyzed Slurry Drop in the Evaporation Region, $x/d = 510$ (Top x 400, Bottom x 3000)	58
22	Droplet Diameter Variation as a Function of Time for the Three Fuels in the Fragation Region, $x/d = 75$	61
23	Droplet Diameter Variation as a Function of Time for the Three Fuels in the Full Combustion Region, $x/d = 340$	62
24	Droplet Diameter Variation as a Function of a Function of Time for the Three Fuels in the Evaporation Region, $x/d = 510$	64
25	Baseline Combustor Configuration and Airflow Distribution	69
26	Atmospheric Combustor Test Rig	70
27	Baseline Combustor with Reduced Primary Zone Cooling Air	72
28	Measured Wall Temperature Using JP-4 Fuel	73
29	Mod IIA Combustor	76

LIST OF ILLUSTRATIONS

<u>Figure</u>	<u>Title</u>	<u>Page</u>
30	Mod IIB Combustor	77
31	Mod IIIA Combustor with Increased Primary Zone Residence Time	78
32	Mod IIIB Combustor	79
33	Atmospheric Combustor Operating on Carbon-Slurry Fuel	81
34	Baseline ETJ131 Combustor	82
35	Mod I Combustor with Low-Cost Airblast Atomizer	85
36	Mod II Combustor with Low-Cost Airblast Atomizer	87
37	ETJ131 Engine Installed in Test Facility	89
38	AiResearch Model ETJ131 Afterburning Turbojet Demonstrator Engine	90

LIST OF TABLES

<u>Table</u>	<u>Title</u>	<u>Page</u>
1	Carbon Slurries Submitted for Burning	12
2	Properties of Slurries Submitted for Burning	13
3	Effect of Additives on Deflocculation of MT Black in JP-10	20
4	Properties of Test Fuels	27
5	Burner Flame Characteristics	34
6	Summary of Slurry Drop Combustion Regions in the Turbulent Flame	48
7	Summary of Slurry Drop Combustion Regions in the Turbulent Flame	49
8	Summary of Flow Properties at Selected Drop Locations	60
9	Initial Pressure-Rig Test Data with a Vaporizing Nozzle	83
10	Second Pressure-Rig Test Data with Airblast Nozzle	84
11	Third Pressure-Rig Test Data of Mod II Combustor with Airblast Nozzle	86

SECTION I

INTRODUCTION

In direct contrast to manned aircraft, which tend to be gross-weight limited, the development of air-breathing missiles has volume as a salient design criterion. Therefore, it is essential that missile systems utilize a fuel that maximizes energy content per unit volume, resulting in minimum volume fuel tanks and maximum range payoffs. The development of carbon-slurry fuels by the chemical industry offers a high potential for meeting the design and mission objectives for advanced missile applications. However, the anticipated physical characteristics of these fuels, as well as combustion-related characteristics, present particular design and development constraints for the airframe/engine fuel system and combustion system. The development of carbon-slurry fuel blends and a combustion system along with interfacing engine and airframe components must be coordinated. In many cases, these tasks must be conducted in parallel in order to meet time constraints for missile development. The major development areas that must be addressed are (1) formulation of a stable, workable and high-heat release carbon-slurry fuel, (2) development of engine-related control, fuel pumping, fuel metering, fuel atomization and combustion systems, and (3) development of airframe-related flight data logic, fuel tankage, and fuel boost system. Figure 1 presents the major consideration for each development area that must be addressed to develop a compatible fuel and missile system. Note that combustion system development and fuel injector development, while usually considered one major area, are separated because of the importance that must be placed on the injector development with the conditions expected as a result of the physical properties of carbon-slurry fuels.

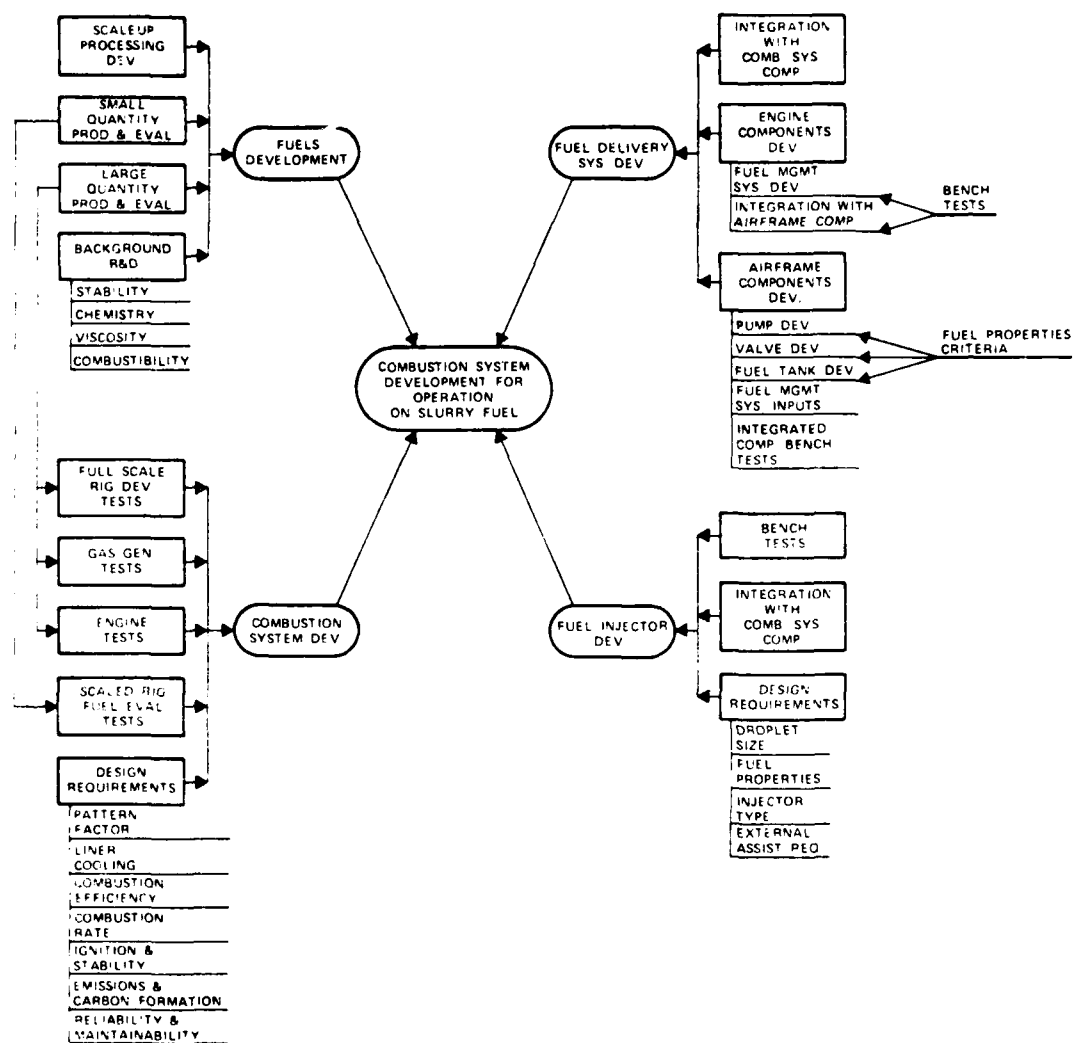


Figure 1. Flow Diagram for Full-Scale Combustion System Development for Operation of Carbon-Slurry Fuel.

The program covered in this report was a five-month technical effort conceived as a preliminary step prior to embarking on a full-scale carbon-slurry fuel development program. The primary objectives of the program effort were to establish the combustibility of a representative carbon-slurry fuel in a turbine engine environment and to determine the major combustion-related development areas that will need to be addressed under full-scale development programs. The emphasis was on obtaining combustion data with fuel development support as necessary to ensure combustibility. As such, the fuel formulations tested were as representative as possible with current technology due to the limited time available. However, some fuel and combustion iterative development was conducted to provide advancements in the fuel state-of-the-art while establishing combustion criteria.

SECTION II

SUMMARY AND CONCLUSIONS

The carbon-slurry fuel evaluation program required demonstrating the feasibility of running a currently available carbon-slurry fuel in a turbine rig and engine in addition to establishing preliminary design criteria for operating on carbon-slurry fuels. The effort consisted of three major interrelated tasks: fuel development and manufacture, fuel droplet measurements, and combustion evaluation. The fuel development and manufacture was conducted under subcontract to Suntech, Inc. The fuel droplet measurement evaluation was conducted under subcontract to Pennsylvania State University. The combustion evaluation tasks were conducted at Garrett-AiResearch. The time constraints imposed by the five-month period of performance for the program dictated that essentially state-of-the-art fuel and combustor hardware be used for the program.

The primary Suntech fuel development effort was to manufacture and supply to AiResearch "burnable" fuel samples for combustion evaluation. Time constraints dictated that the supplied samples have some compromises in order to ensure their combustibility. However, the intent was to supply samples that were as representative as possible with regard to physical properties that can be expected in ultimate fuel specifications. This approach supported the ability to determine the preliminary criteria necessary to operate a turbine engine combustor successfully on carbon-slurry fuel. However, some fuel development was attained in the program. The initial fuel samples were run in an AiResearch atmospheric combustion rig, and the data from these tests was factored into iterating the subsequent fuel samples. This provided for adjustment to the carbon loading and the addition of a catalyst and other additives to improve the fuel combustibility and rheological properties. After limited fuel/combustion iterations, a slurry formulation (consisting of

approximately 50 percent by weight of medium thermal (MT) carbon black in a JP-10 carrier with a catalyst and additive package to promote acceptable rheology stability was identified. Thirty gallons of this formulation were delivered to AiResearch for combustion rig and demonstration-engine testing.

Suntech conducted a parallel activity during the fuel manufacture that sought to identify the variables that would allow a stable slurry to meet the target specifications. This effort was comprised of a study to determine the effects of varying additive packages (deflocculants, dispersants, and viscosity aids) on fuel rheology and stability. Several slurry formulations were studied and measurements were obtained on viscosity characteristics. The study indicated that for the substances evaluated, on an equal weight basis, the dispersant had little effect on the rheological characteristics of the fuel while the deflocculants had the greatest effect and the viscosity aids a secondary effect. More work is needed to optimize the contents and amounts of the additive packages and characterize the fuel samples with varying amounts of carbon loadings. In addition, major efforts will be required to improve the long-term stability and raise the heating value while maintaining acceptable rheological properties.

The fuel droplet measurement evaluation conducted at Pennsylvania State University sought to make a preliminary investigation into the fuel breakdown prior to combustion, the droplet behavior in the combustion process, and the nature of the residue remaining following combustion. The droplet combustion process is fundamental to successful operation in a combustor since it affects the residence time requirement and combustion efficiency in the combustor. The preliminary work conducted in this program was done with supported droplets suspended in a turbulent flame. The droplets were considerably larger than the droplets formed with an air blast fuel nozzle typical of gas turbine combustion systems, but the qualitative observations are considered useful

for preliminary design purposes. The phenomena observed confirmed the theory that the liquid fuel carrier burns off quickly followed by the reaction of the carbon. The study also included evaluation of the residue remaining after combustion. The effects of using a combustion catalyst indicated that a more complete reaction could be obtained over a wider burning range. Future work will need to be conducted to extend the evaluation to droplets that are closer to the expected airblast droplet size. This will permit quantitative burning rates to be established that will provide design criteria for the residence time and air staging requirements for the gas turbine combustor.

The combustion testing conducted at AiResearch consisted of the evaluation of three slurry-fuel samples supplied by Suntech in combustion rig and demonstration engine environments. The time limitations constrained the combustion evaluation to only limited iterative hardware development on conventional existing hardware.

The combustion testing was conducted first in test rigs, and finally in an AiResearch ETJ131 Turbojet Engine. The initial combustion rig testing was conducted on an atmospheric rig that permitted visual inspection of the combustor flame and exhaust. Limited fuel and combustion hardware iteration provided for the selection of a fuel formulation and combustor configuration for subsequent testing. During this testing, the staged burning nature of the fuel and the need for a combustion catalyst to enhance burning were identified. Subsequent rig testing was in a pressure facility that permitted more quantitative evaluations to be made. The combustion system from the ETJ131 demonstrator engine was utilized for the pressure rig evaluations. Several hardware modifications were made during this testing. A combustion efficiency of 92 percent was obtained with the selected carbon-slurry formulation. Time constraints again precluded further modifications to improve the efficiency but it could be

expected that normal development could raise the efficiency to acceptable levels. Smoke levels were higher for the slurry than JP-4 because of the lower efficiency. There was no carbon buildup on any of the combustor components following the testing. The final combustor configuration from the pressure rig testing was installed in the ETJ131 Engine for engine testing.

Approximately thirty-five minutes of run time on carbon-slurry fuel was accumulated on the ETJ131 Engine. The engine had no operational problems, and no excessive temperature levels were noted. The noticeable smoke was considered to be due primarily to the combustion inefficiency, which could be reduced through normal development. Upon completion of the testing, no carbon deposits were observed on any of the engine components.

Based upon the limited combustion testing conducted under this program, the outlook for optimizing gas turbine combustion systems to operate on carbon-slurry fuels is encouraging. Fuel delivery and control systems will require extensive development to accommodate the rheology and stability properties of the ultimate specification fuels, especially at low-temperature operation. Fuel atomization development will be critical to obtain the capability of optimum droplet sizes. The critical combustion technology requirement will be to optimize the combustor aerodynamics to accommodate the dual burning nature of slurry fuels. This will be necessary to obtain successful complete combustion of the carbon, and hence, obtain acceptable combustion efficiencies. Ignition capability with a carbon slurry will be another challenging area that will require development, especially for airblast fuel injectors, which have limited atomization capability at starting conditions. All of the development areas identified in this program are considered to be achievable within the scope of a combustion development program.

SECTION III

TECHNICAL DISCUSSION

1. Fuel Development

a. Fuel Development Background

The carbon-slurry fuel development and formulation of slurries suitable for burning were conducted under subcontract to Suntech, Inc. The principle objective was first, to supply sufficient quantities of a "burnable fuel" for assessing combustion characteristics, and secondly, to identify those variables that affect slurry viscosity, slurry stability, and the effect of catalyst on burning rate. The time period in which the work was conducted required that a suitable, but not an optimum, formulation be developed rapidly and submitted to AiResearch for combustion evaluation. The formulation selected for the burning tests was, therefore, a compromise. It resulted in a reasonably stable dispersion of large particle size medium thermal (MT) black in JP-10. The formulation contained additives to deflocculate the black, stabilize the dispersion, and promote combustion. The solids content was fixed at 50 percent by weight so that slurry viscosity would remain under 50 centipoises. Even at this concentration, the targeted 180,000 Btu/gallon was not obtained.

Parallel slurry development work was conducted to identify the fuel formulation variables that would allow a stable combustible slurry to be achieved that meets the target heat content.

b. Slurry Formulation, Preparation, and Characterization

(1) Slurry Formulation

The slurries were prepared by dispersing medium thermal (MT) black in JP-10, exo-tetrahydrodi(cyclopentadiene). Carbon black was supplied by the Huber Corporation, and JP-10 was manufactured by Suntech. Carbon blacks are highly agglomerated and surfactants are required to effect deflocculation and to maintain the deaggregated particles in the dispersed state. Carbon black, like graphite, is difficult to oxidize. Unlike coal, it has no volatile materials that are released as the temperature of the mass is increased, which helps to sustain combustion. However, it has been found, according to the literature, that there are various materials that have been demonstrated to lower the ignition temperature and increase the rate of oxidation.

Literature on the preparation of carbon dispersions suggested the use of a basic nitrogen-containing surfactant to deflocculate the particles and the use of a calcium or barium petroleum sulfonate as the dispersant. A succinimide oligomer manufactured by Edwin Cooper was chosen as the deflocculating agent. The petroleum sulfonate was supplied by Witco as the calcium salt. The literature also reports that the natural resin, Gilsonite, is highly effective in reducing the viscosity of carbon black dispersions. Gilsonite (Zeco 11-4) was obtained from the Ziegler Chemical and Mineral Company. The catalyst consisted of a soluble lead compound furnished by the Mooney Chemical Company as lead neodecanoate or methylcyclopentadienyl manganese (MMT) supplied by the Ethyl Corporation.

No attempt was made to optimize the additive package because of time limitations. The formulated dispersion did have the viscosity characteristics desired for fuel handling and atomization and sufficient short-term stability to maintain a uniform dispersion during the duration of the combustion tests. Further development work will be required to obtain long-term stability of the dispersions.

(2) Slurry Preparation

Slurries were prepared by making a premix (carbon black, JP-10, and surfactants) utilizing a Premier Mill high-speed laboratory dispersator, operating at 15,000 rpm. A weighed quantity of JP-10 plus additives was placed in a stainless steel vessel and the carbon black added in increments until the required solids level had been reached. Deflocculation of carbon particles was achieved by the selection of proper additives, coupled with mechanical shear.

The final step in the slurry preparation was that of ball milling or grinding in a continuous media mill. The ball mill utilized 1.9-cm steel balls in a ceramic jar, and milling was allowed to proceed for 16 hours. The media mill (sometimes called a sand mill) utilized 1- to 3-mm zirconium beads. Residence time in the mill was 20 minutes, obtained by recycling the slurry a total of four passes.

(3) Slurry Characterization

Solids content of the slurries was determined gravimetrically. A weighed sample of the slurry was placed in an air oven for 16 hours at 398K and the weighed residue represents the carbon content of the slurry plus the nonvolatile additives. A correction was therefore made for the additives considered to be nonvolatile in calculating the carbon content of the slurry.

Both the Brookfield viscometer and the Haake precision rotating cylinder viscometer were utilized in measuring the flow characteristics of the slurries. The Brookfield was operated at ambient temperature. The Haake viscometer was operated at controlled temperature.

Slurry density was measured utilizing a pycnometer or a Mettler density meter.

Heats of combustion were obtained in a Parr calorimeter according to ASTM Test Method D240-76.

The use of the scanning electron microscope (SEM) to determine the degree of carbon particle deflocculation was found to be unsatisfactory. The diluted dispersions reagglomerated during preparation of the sample for the SCM.

(4) Slurries Submitted for Burning Tests

Table 1 tabulates the carbon slurries consisting of MT black dispersed in JP-10 that were supplied by Suntech for burning in various combustion rigs. Table 2 tabulates the properties of these slurries. Figure 2 is a plot of the shear stress as a function of the shear rate for a slurry of 50-percent MT black in JP-10 at ambient temperature. The flow behavior appears to be Newtonian. In Figure 3, an ASTM Viscosity Temperature Chart has been used to plot the viscosity of a 50-percent slurry as a function of temperature. Extrapolation, which may not be valid, yields a viscosity of 700 cP at 219K.

c. Slurry Development Program

Concurrent with the program to furnish carbon-slurry fuel for burning in various test rigs and finally in a turbine engine, Suntech also engaged in a slurry-fuel development program. The objective of the development program was to identify those parameters that influence the rheological properties of carbon slurries so that a transportable fuel, meeting the target heat of combustion of 180,000 BTU/gallon, could be formulated and utilized in future programs.

TABLE 1
CARBON SLURRIES SUBMITTED FOR BURNING

Sample No.	Date	Amount in Gallons	Liquid Phase	Solid Phase	% Solid	% Additive Based on Solid Phase				Combustion Additive
						Cooper Hitec E-645	Gilsonite Zeco 11-A	Witco Petronate 25-C		
790-928	5-21-79	2	JP-10	MT Black	50	2.0	2.0	2.0	--	--
790-942	6-18-79	1	"	"	50	1.0	1.0	1.0	1.0% Pb (1)	1.0% Pb (1)
790-957	7-13-79	1	"	"	40	1.0	1.0	1.0	5.0% MMT	5.0% MMT
790-958	7-13-79	1	"	"	40	1.0	1.0	1.0	3% Pb (1)	3% Pb (1)
790-959	7-13-79	1	"	"	50	1.0	1.0	1.0	1.0% Pb (3)	1.0% Pb (3)
790-969	7-27-79	3-1/2	"	"	50	2.0	2.0	2.0	1.0% Pb (1)	1.0% Pb (1)
790-971	8-4-79	1	"	"	65	Second Footnote (2)				
790-974	8-29-79	30	"	"	50	2.0	2.0	2.0	1.0% Pb (1)	1.0% Pb (1)

Footnote:

- (1) Pb as Mooney TEN-CHEM - 24% Pb
 (2) Additive Package based on black - 1.85% Lubrizol 2155, 3.7% Lubrizol 2153, 1% Pb
 (3) 25% of JP-10 replaced by Sunpar 120 (Paraffinc Oil), Pb as Mooney NAP-All-24% Pb

TABLE 2
PROPERTIES OF SLURRIES SUBMITTED FOR BURNING

Sample No.	Carbon Content Wt. %	Density g/cm ³	Hc BTU/Gal.	Viscosity Centipoise Haake	Wt. % Pb	Wt. % Mn	Note
790-928	50.4	1.244	168,859	26 at 27°C	--	--	Prepared on Ball Mill
790-942	49.2				0.45	--	"
790-957	42.6				--	0.52*	Prepared on Media Mill
790-958	39.95				1.4*	--	"
790-959	49.45				0.6*	--	"
790-969	49.8			40 at 25°C	0.6*	--	"
790-971	63.8	1.343	176,983		0.6*	--	"
790-974-1	50.1	1.2364	167,564	58±	0.3	--	"
-2	50.1			63±	0.6*	--	"
-3	49.9			63±	0.6*	--	"
-4	50.0	1.24*	170,000*	46±	0.6*	--	"
-5	50.0			42±	0.6*	--	"
-6	50.3			75±	0.6*	--	"

* Calculated or estimated values

± Brookfield - apparent viscosity at 60 RPM, Spindle #2, Ambient Temperature

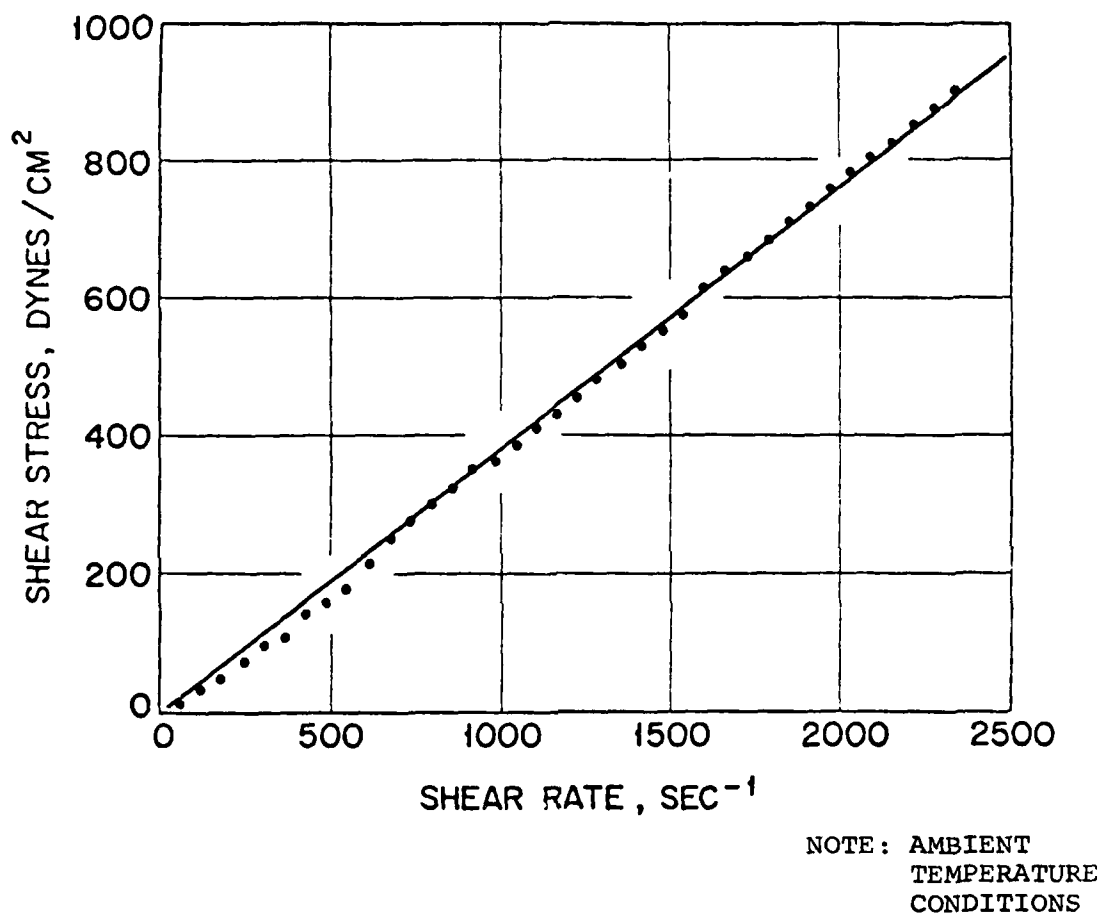


Figure 2. Shear Rate Versus Shear Stress for Sample of 50 Percent by Weight of MT Black in JP-10.

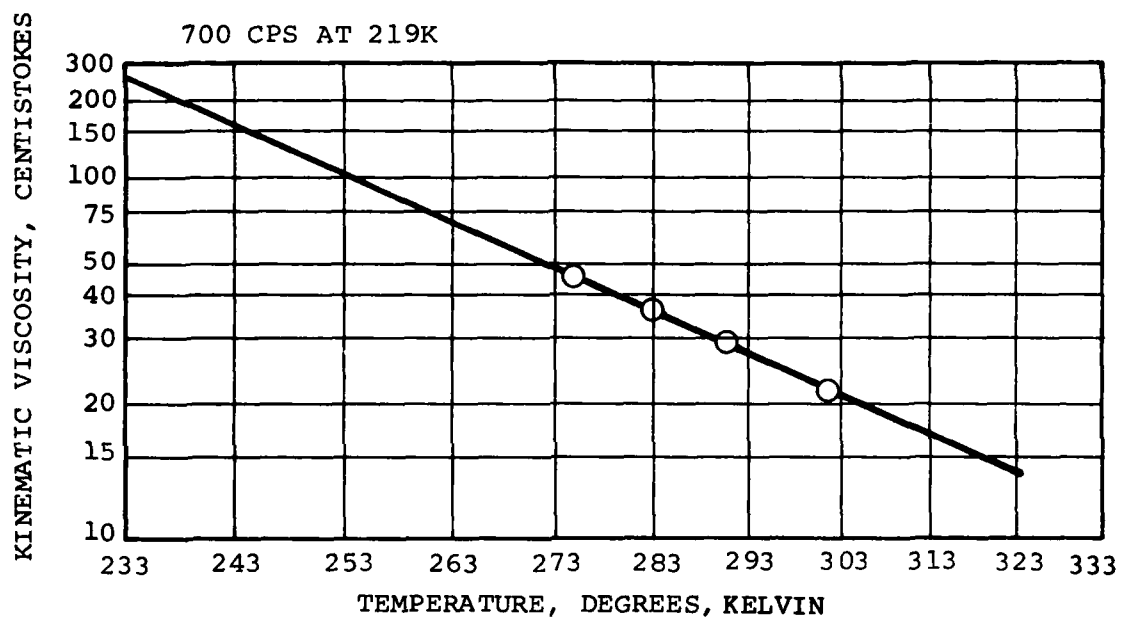


Figure 3. Viscosisty-Temperature Chart for Sample 790-928
(50 Percent by Weight of MT Black in JP-10).

(1) Formulations with Varied Additive Package Components

The baseline slurry fuel contained three components. Component A is designated as the deflocculant (Hitec E645), Component B is designated as a dispersant (Petronate 25-C), and Component C is designated as responsible for reducing the viscosity (Gilsonite). These materials were utilized in the ratio A:B:C = 1:1:1 with each component added at the two-percent level with respect to the concentration of black. In order to determine the function of the components of the additive package and to arrive at an improved formulation, a series of some thirty slurries of MT black at the 50-percent level in JP-10 were prepared in which the additives were varied over a wide range.

The slurries were prepared utilizing the high-speed stirrer only, omitting the use of the media mill. This was done since screening experiments demonstrated that there was no change in the Brookfield viscosity for those slurries processed in the media mill, in addition to 60 minutes of shear in the high-speed stirrer. This does not mean that there is no further reduction in particle agglomeration in the media mill, only that the Brookfield viscosity is not affected.

(2) The Use of the Brookfield Viscometer to Characterize Slurries

The Brookfield viscometer was utilized to characterize all slurries. Measurement was made at ambient temperature in containers where the diameter of the container was large compared to the diameter of the spindle.

The Brookfield viscometer operates at very low rates of shear, and the shear strain is of the order of 5 sec^{-1} at the highest shear rate, which is at 60 rpm. The low rate of shear is a consequence of the fact that the radius of the rotating spindle is small compared to the radius of the container in which the

measurements are made. However, for the purpose of this program, this low shear strain was very useful in that it allowed weak-bridged carbon structures in the dispersion--formed as a result of particle interaction--to be identified, and their magnitude estimated.

All dispersions examined in this study were pseudoplastic with a yield point. It was found that the torque read on the Brookfield viscometer increased with the shear rate according to the following equation:

$$f = a(1 + \text{rpm})^b \quad (1)$$

where f is the torque in scale units, rpm is the rate of rotation of the spindle and a and b are constants. Equation (1) can be written

$$\log f = \log a + b \log (1 + \text{rpm}) \quad (2)$$

where a is the intercept and b the slope of the line obtained by plotting $\log f$ against $\log (1 + \text{rpm})$. The extent to which the data fit Equation (2) is demonstrated in Figure 4 for several dispersions. If the fluid has no structure, $\log a$ will be small, and b will be unity--i.e., a Newtonian fluid. The value of a is the "yield point" and represents the extent of the structure at rest. The value of b is an indication of how easily the structure is broken down under shear. The lower the value of b , the less stable the structure. A third quantity of interest is the apparent viscosity, η' , defined as:

$$\eta' = \frac{f_i - a}{\text{rpm}_1} G \quad (3)$$

where f_i is the measured torque at a given rpm, and the constant G is used to convert the readings to centipoise. For the instrument used, the value of G was determined to be 50 for spindle No 1, 250 for spindle No. 2, and 1000 for spindle No. 3.



AIRESEARCH MANUFACTURING COMPANY OF ARIZONA
A DIVISION OF THE GARRETT CORPORATION
PHOENIX, ARIZONA

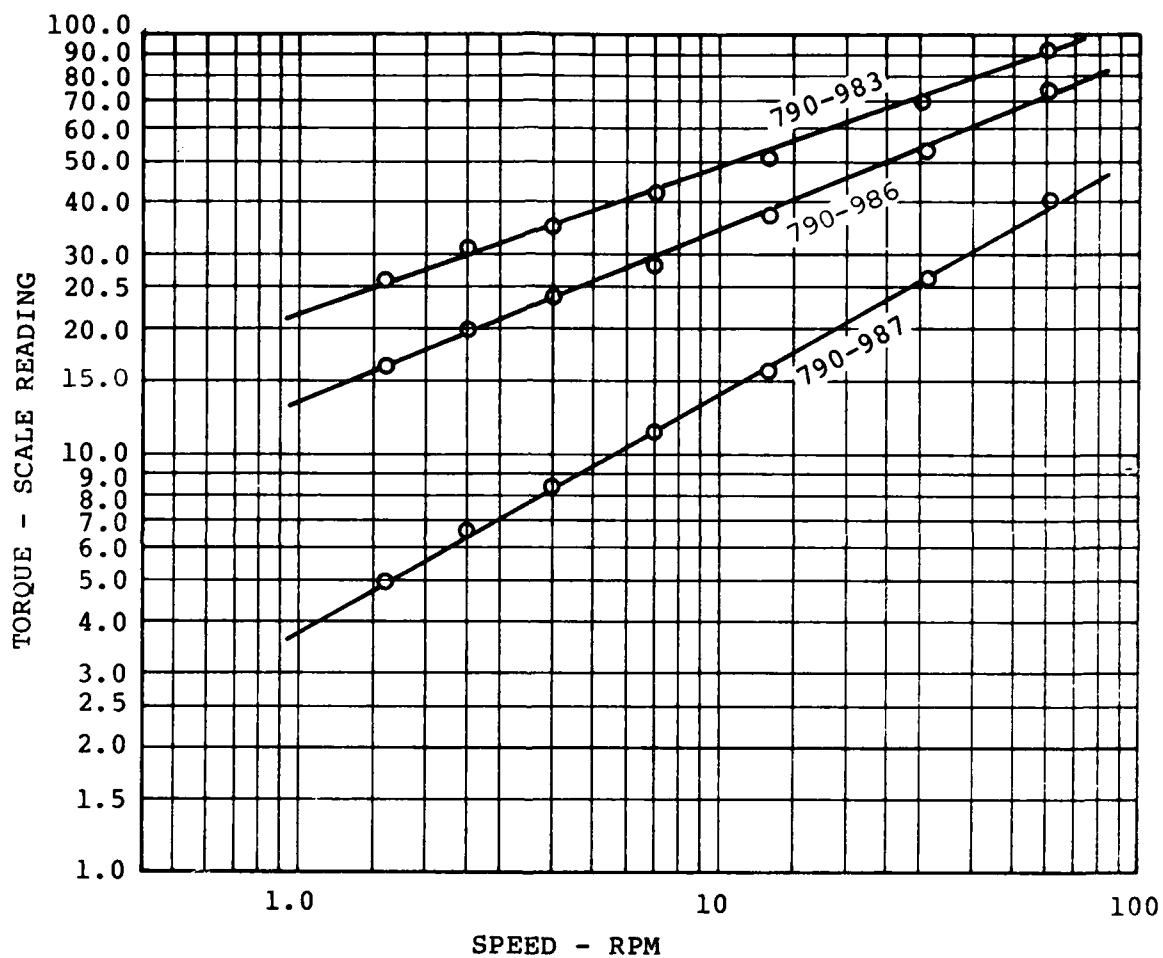


Figure 4. Torque and Speed Relationships for Determining Brookfield Viscosity.

The apparent viscosity will increase at a constant carbon loading as the structure and degree of particle flocculation in the dispersion increases due to immobilization of the liquid in particulate networks.

The dispersion may conveniently be ranked by combining, η' , a , and b to yield a "figure of merit" defined as:

$$M = \frac{\text{Slope}}{\text{viscosity} \times \text{yield point}} = \frac{b}{\eta' \times a} \times 10^3 \quad (4)$$

d. Results of Components of the Additive Packages on Rheological Properties of Slurries.

All data collected on the effect of the components studied to deflocculate and disperse the carbon black in JP-10 are summarized in Table 3 utilizing the procedures discussed in the previous paragraph.

The values listed in Table 3 demonstrate that Component B, the calcium sulfonate (Witco Petronate 25C), is not necessary in the formulation and is, in fact, detrimental. Also, it will be found that Component C, the Gilsonite Zeco 11A, is not as effective as Component A, the polymeric succinimide (Cooper Hitec E-645), on an equal weight basis. Accordingly, the best formulation of those examined to effect deflocculation is a nitrogen-containing material such as Cooper Hitec E-645 or Lubrizol 2153.

There remains to be determined the minimum level of additive to obtain the maximum degree of deflocculation in MT black. This can be accomplished by examining the effect of the concentration of Component A on the value of η' , a , and b . Figure 5 demonstrates that the viscosity decreases (the fluidity increases) with the amount of Component A added, leveling off at a concentration >3 percent. Figure 6 is a plot of the "yield points" a , as a function of concentration, and Figure 7 is a plot of the torque-rpm slope b as a function of concentration of Component A.

TABLE 3. EFFECT OF ADDITIVES ON DEFLOCCULATION OF MT BLACK IN JP-10.
(50% BLACK DISPERSED IN JP-10)

Sequence Number	Experiment Number	% Component A	% Component B	% Component C	C (% Total Additive on Black)	Brookfield Viscosity				M	M/C
						Intercept	Slope	Torque Scale 60 rpm	η		
1	790-983	1.0	--	--	1	21.2	0.36	91	50	0.34	0.34
2	790-984	--	--	--	1	400.0	0.51	960	467	0.003	0.003
3	-985	--	--	--	1	115.0	0.24	320	171	0.012	0.012
4	-986	1.0	1.0	--	2	13.5	0.40	75	51	0.58	0.29
5	-987	1.0	--	--	2	3.7	0.58	40	30	5.26	2.60
6	-988	--	--	--	2	75.0	0.17	230	129	0.027	0.14
7	-989	1.0	1.0	--	3	8.1	0.52	68	50	1.28	0.43
8	-990	0.5	0.5	--	1.5	21.5	0.35	91	58	0.28	0.19
9	-991	2.0	0.5	--	3.0	6.0	0.47	41	29	2.7	0.90
10	-992	0.5	0.5	--	3.0	22.0	0.36	97	63	0.26	0.09
11	-993	2.0	0.5	--	4.5	6.6	0.38	46	33	1.75	0.39
12	-994	0.5	0.5	--	3.0	3.6	0.66	54	42	4.3	1.45
13	-995	2.0	2.0	--	4.5	4.0	0.58	46	35	0.42	0.93
14	-996	0.5	2.0	--	4.5	4.3	0.66	65	51	3.0	0.67
15	-997	2.0	2.0	--	6.0	4.0	0.59	46	35	4.16	0.69
16	791-005	0.5	--	--	0.5	108.0	0.24	291	152.5	0.015	0.03
17	-006	2.0	--	--	2.0	3.2	0.62	39.9	30.6	6.25	3.12
18	-007	4.0	--	--	4.0	2.6	0.62	31.5	24.1	9.9	2.5
19	-008	1.0	--	--	1.5	16.8	0.49	126.0	91.0	0.32	0.21
20	-009	1.0	--	--	3.0	2.5	0.67	39.5	30.8	8.3	2.8
21	-010	2.0	2.0	--	4.0	3.1	0.57	46.9	36.5	5.0	1.25
22	-011	4.0	--	--	6.0	2.8	0.65	39.6	30.7	7.7	1.28
23	-012	2.0	2.0	--	2.0	4.2	0.59	48.5	36.9	3.8	1.9
24	-013	2.0	Cooper Hitec E - 644	--	2.0	3.1	0.66	41.0	38.5	5.6	2.8
25	-014	2.0	Cooper Hitec E - 638	--	2.0	144.0	0.27	452.0	257.0	0.007	0.0035
26	-015	2.0	Lubrizol 2152	--	2.0	2.6	0.65	38.0	31.7	7.7	3.85
27	-016	2.0	Lubrizol 2153	--	2.0	6.4	0.53	55.0	45.9	1.8	0.90
28	-018	0.75	Lubrizol 2155	--	0.75	55.0	0.26	160.0	87.3	0.054	0.072
29	-019	1.5	--	--	1.5	11.2	0.43	66.0	45.7	0.84	0.56
30	-020	10.0	--	--	10.0	3.3	0.61	35.0	26.4	7.0	0.69

Components:

- A - Cooper Hitec E-645
- B - Witco Petronate 25C
- C - Gilsonite Zeco 11A

BROOKFIELD VISCOSITY - 50% MT BLACK IN JP-10
 $\eta^1 = [(\text{TORQUE 60 RPM} - \text{INTERCEPT})/\text{RPM}]^{50}$

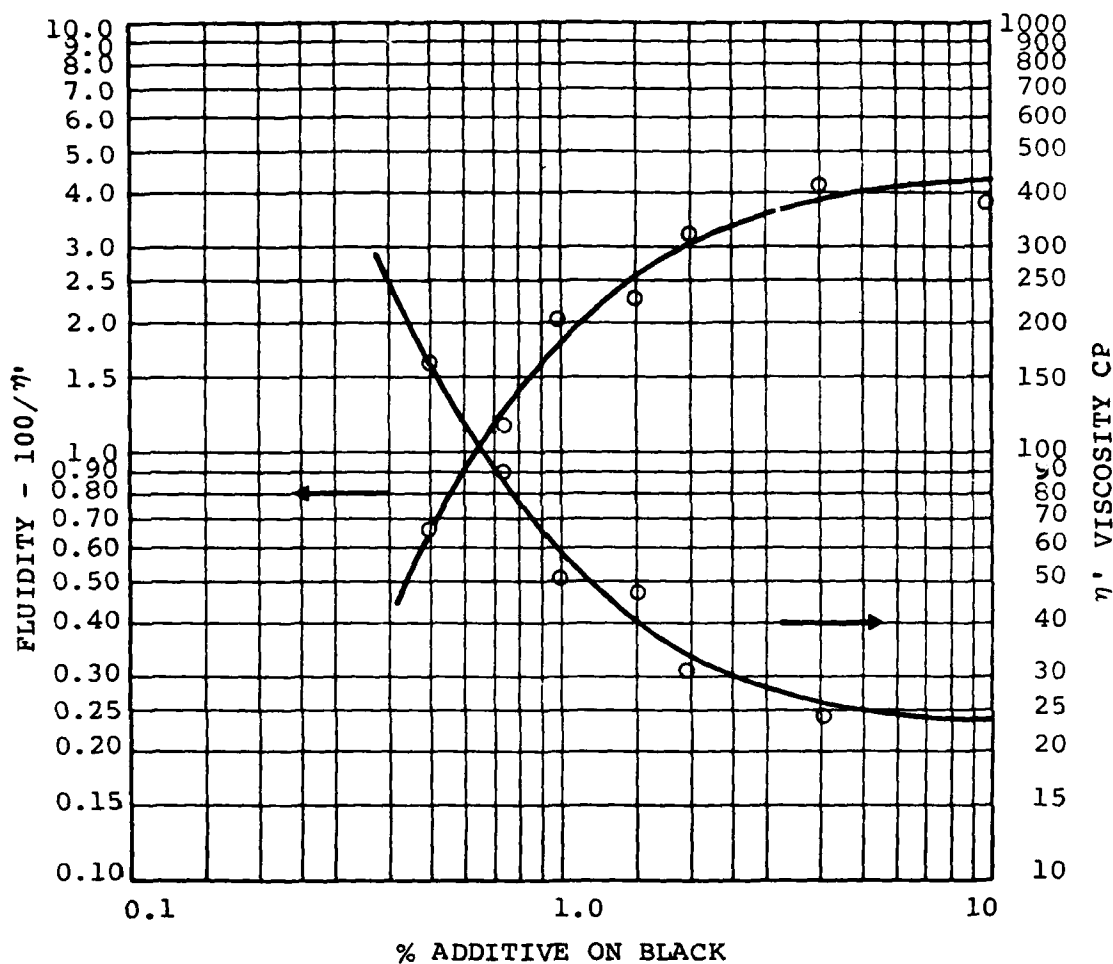


Figure 5. Fluidity as a Function of Percent MT Black.

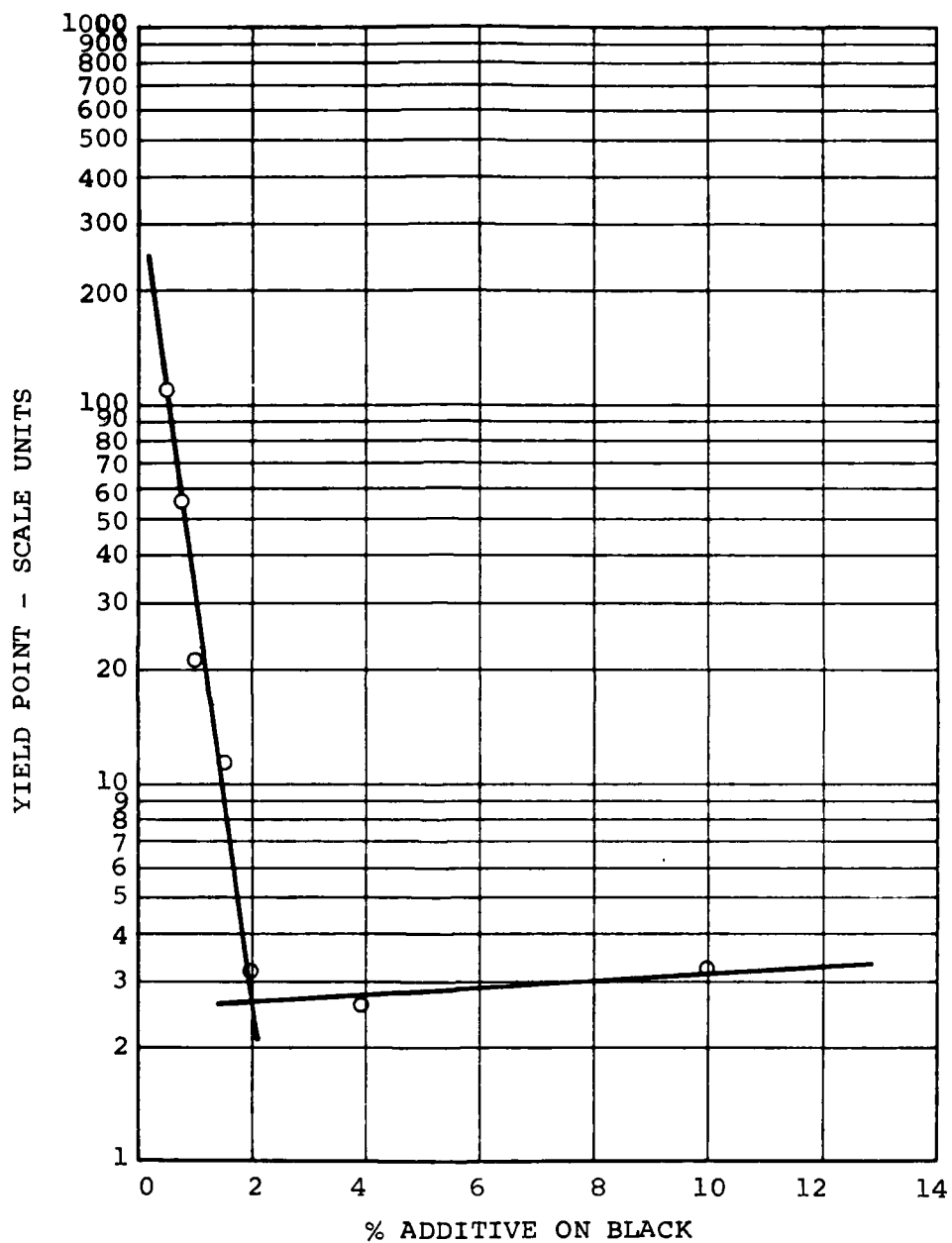


Figure 6. Yield Point as a Function Additive Concentration (50-Percent Black in JP-10).

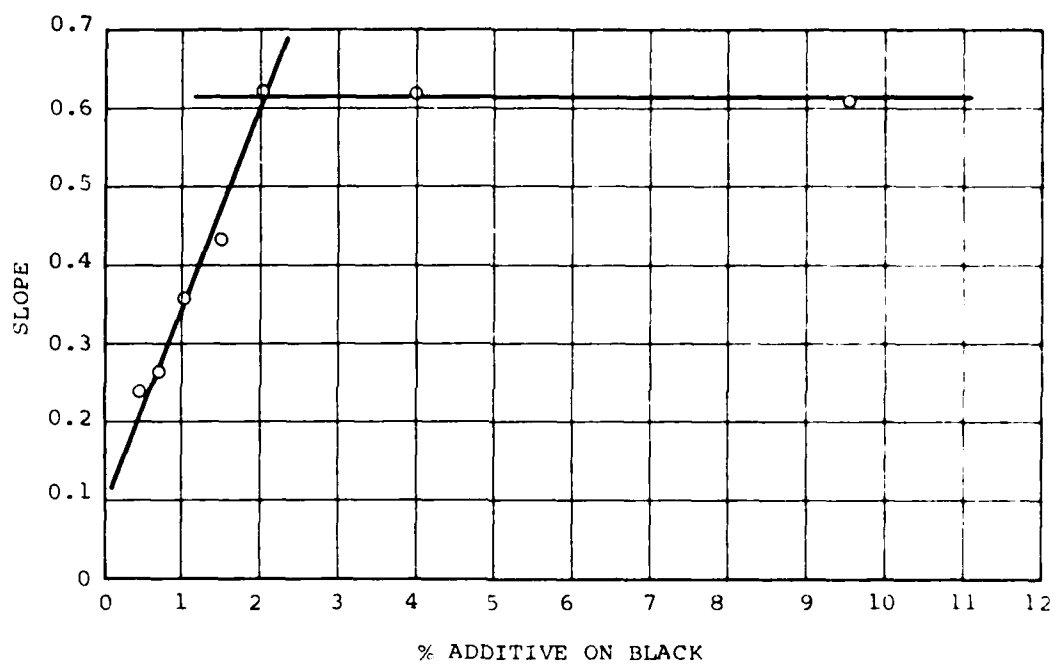


Figure 7. Component A on MT Black in JP-10 Effect of Concentration on Torque/RPM Slope (50-Percent) Black in JP-10).

Both a and b appear to show distinct break points at a 2-percent concentration level. It is likely that at this level, the MT black has become saturated with adsorbed polymeric succinimide. Therefore, three to five percent of Component A, based on concentration of MT black in the dispersion, is sufficient to give the maximum degree of particle deflocculation consistent with the amount of shear energy applied in the mixing process. Note that this data applies to Cooper Hitec E-645 only and does not rule out the possibility that more efficient compounds may be identified.

Finally, in Figure 8 "figure of merit", M, is plotted as a function of additive concentration for three systems. This data again demonstrates that Component A is most effective and that the three-component system used to prepare the slurry for demonstration of burning efficiency was a good first choice, although not necessarily the optimum.

2. Fuel Droplet Measurements

A subcontract was issued to Pennsylvania State University to conduct carbon-slurry fuel droplet evaporation/combustion characteristics. This work was conducted under the direction of Professor G. M. Faeth assisted by Mr. G. A. Szekely Jr. The studies utilized JP-10 as a baseline since that is the carrier fuel utilized in the slurry samples formulated to date. In addition, JP-10 was used for the carbon-slurry formulation samples identical to those delivered by Suntech under subcontract to AiResearch for combustion evaluation.

a. Fuel Droplet Measurement Background

The carbon-slurry fuel samples evaluated consisted of a medium thermal carbon black with JP-10 as the liquid carrier fuel. The properties of the three fuels considered during this

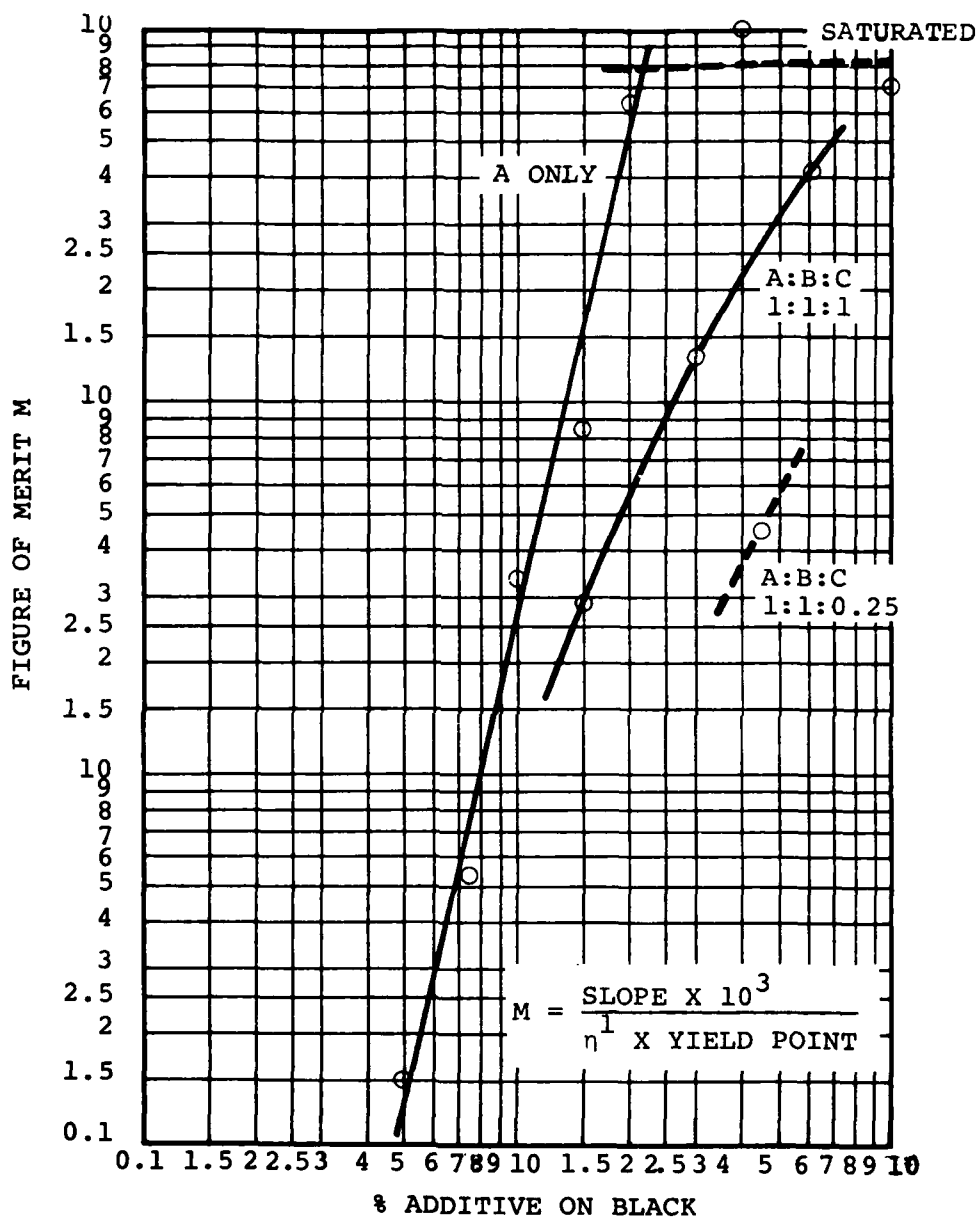


Figure 8. Effect of Additive Composition and Concentration of Deflocculation of MT Black in JP-10.

study are summarized in Table 4. As a baseline, pure JP-10 was studied. Two slurry fuels were also examined with weight percentages for carbon of approximately 50 percent. One of these slurries incorporated a catalyst to facilitate the reaction of the carbon (Ref. 1). The ultimate carbon particle size in both cases was $0.3\text{ }\mu\text{m}$. Other properties of the slurry fuels are discussed in Ref. 2.

Slurries have not been widely used in the past, and the existing literature on their combustion characteristics is limited. A recent paper by Law, et al. (Ref. 3) reports some results on the combustion characteristics of single supported slurry droplets. Combustion was undertaken in still air under natural convection conditions. The slurry consisted of dried, 200 mesh, coal powder (coal type unidentified) in No. 2 heating oil. The droplets were supported from a small probe (initial drop diameters of 850 to 1250 μm) and ignited. The initial combustion process was fueled by the liquid. As the liquid continued to evaporate, small masses of material (presumably containing coal particles) were intermittently ejected from the probe. After all the oil had vaporized, the flame extinguished, leaving an irregularly shaped agglomerate of coal particles on the support. The mass of material remaining on the probe increased as the initial percentage of coal in the slurry was increased. For initial coal weight percentages greater than 15 to 20 percent, the mass of the coal agglomerate remaining after extinction reached 70 to 80 percent of the initial mass of coal in the drop.

1. R. S. Stearns, personal communication, June 20, 1979.
2. T. W. Bruce, H. C. Mongia, R. S. Stearns, L. W. Hall and G. M. Faeth, "Formulation Properties and Combustion of Carbon-Slurry Fuels," Sixteenth JANNAF Combustion Meeting, Naval Postgraduate School, Monterey, CA, September, 1979.
3. C. K. Law, C. H. Lee and N. Srinivasan, "Combustion Characteristics of Water-in-Oil Emulsions and Coal-Oil Mixtures," Paper No. 38, 1978 Fall Technical Meeting, Eastern Section of the Combustion Institute, Miami Beach, Florida, November, 1978.

TABLE 4. PROPERTIES OF TEST FUELS¹

	Base Fuel	Noncatalyzed Slurry	Catalyzed Slurry ²
Designation	-	790-928	790-942
Liquid	JP-10	JP-10	JP-10
Dispersed Carbon ³ (wt. %)	-	50.4	49.2

¹All fuels supplied by R. S. Stearns, Suntech, Inc.,
P. O. Box 1135, Marcus Hook, PA 19061.

²The catalyst is a proprietary lead compound [1].

³The dispersed carbon is a medium thermal carbon (MT black)
having an ultimate particle size of 0.3 μ m. Further
properties of this material are provided in Ref. 2.

Based on existing information on coal combustion (Reference 4 through 8), it is likely that persistent combustion of a coal slurry droplet in air involves three major processes: (1) evaporation and combustion of the liquid fuel, (2) devolatilization of the coal with subsequent oxidation, and (3) reaction of the remaining solid carbon/ash particle. In contrast, the present slurry fuels employ carbon black as the solid phase and a devolatilization stage is not expected. Judging from the results of Ref. 3, carbon levels in the present test slurries are sufficiently high to result in significant agglomeration.

The investigation described herein involved a brief preliminary study of the combustion characteristics of the fuels listed in Table 4. The experimental method involved observing the combustion of single supported fuel droplets, in both still air and in a turbulent diffusion flame. The latter condition was examined in order to better simulate the local environment of droplets within a combustion chamber. Similar to the results for coal slurries (Ref. 3), agglomerates remained on the drop support following combustion. The structure of these agglomerates was studied using a scanning electron microscope (SEM). Combusting droplets were also observed using dark field and shadowgraph motion pictures. These data were reduced to yield particle diameter as a function of time and burning rates.

-
4. J. L. Krazinski, R. O. Buckius, and H. Krier, "Coal Dust Flames: A Review and Development of a Model for Flame Propagation," Prog. Energy Combust. Sci. 5, 31, 1979.
 5. M. F. R. Mulcahy, I. W. Smith, Rev. Pure Appl. Chem. 19, 81, 1969.
 6. P. L. Walker, F. Rusinko, L. G. Austin, Adv. Catal. 11, 134, 1959.
 7. D. Gray, J. G. Cogoli, R. H. Essenhigh, Adv. Chem. Ser., No. 131, p. 72, 1973.
 8. M. A. Field, D. W. Gill, B. B. Morgan, and P. G. W. Hawksley, "Combustion of Pulverized Coal," BCURA Leatherhead, Cherey and Sons, LTD., Banbury, England, 1967.

b. Fuel Droplet Experimental Program Description

(1) Apparatus

The test apparatus involved modification of an earlier arrangement employed for a study of gas and spray diffusion flames (References 9 through 11). A sketch of the apparatus appears in Figure 9. The arrangement consists of an injector flowing propane gas, which is burned as a diffusion flame in stagnant room air. The test droplet is supported from a probe at various locations in the flame and photographed with a motion picture camera.

The gas injector was positioned near the bottom of the test stand and oriented vertically upward. The test stand has an area 1.44-m^2 square and 3.0-m high enclosed with a single thickness of 16-mesh screen. The test stand was located within a room having dimensions 4 m x 7 m x 4-m high. Combustion products were removed through an exhaust fan located near the ceiling of the test cell. The injector was seated on a support that allowed a vertical movement of 1.2 m. Two traversing mechanisms were used to position the nozzle in the horizontal plane.

The nozzle was a full-cone air atomizing injector, with no swirl, manufactured by the Spray Systems Company (model 1/4 J 2050 fluid nozzle and model 67147 air nozzle). The outlet diameter of the nozzle was 1.194 mm.

9. C-P. Mao, G. A. Szekely, Jr. and G. M. Faeth, "Evaluation of a Locally Homogeneous Model of Spray Combustion," NASA CR-3202, November, 1979.
10. A. J. Shearer and G. M. Faeth, "Evaluation of a Locally Homogeneous Model of Spray Evaporation," NASA CR-3198, October, 1979.
11. A. J. Shearer, H. Tamura and G. M. Faeth, "Evaluation of a Locally Homogeneous Flow Model of Spray Evaporation," AIAA J. Energy, in press.

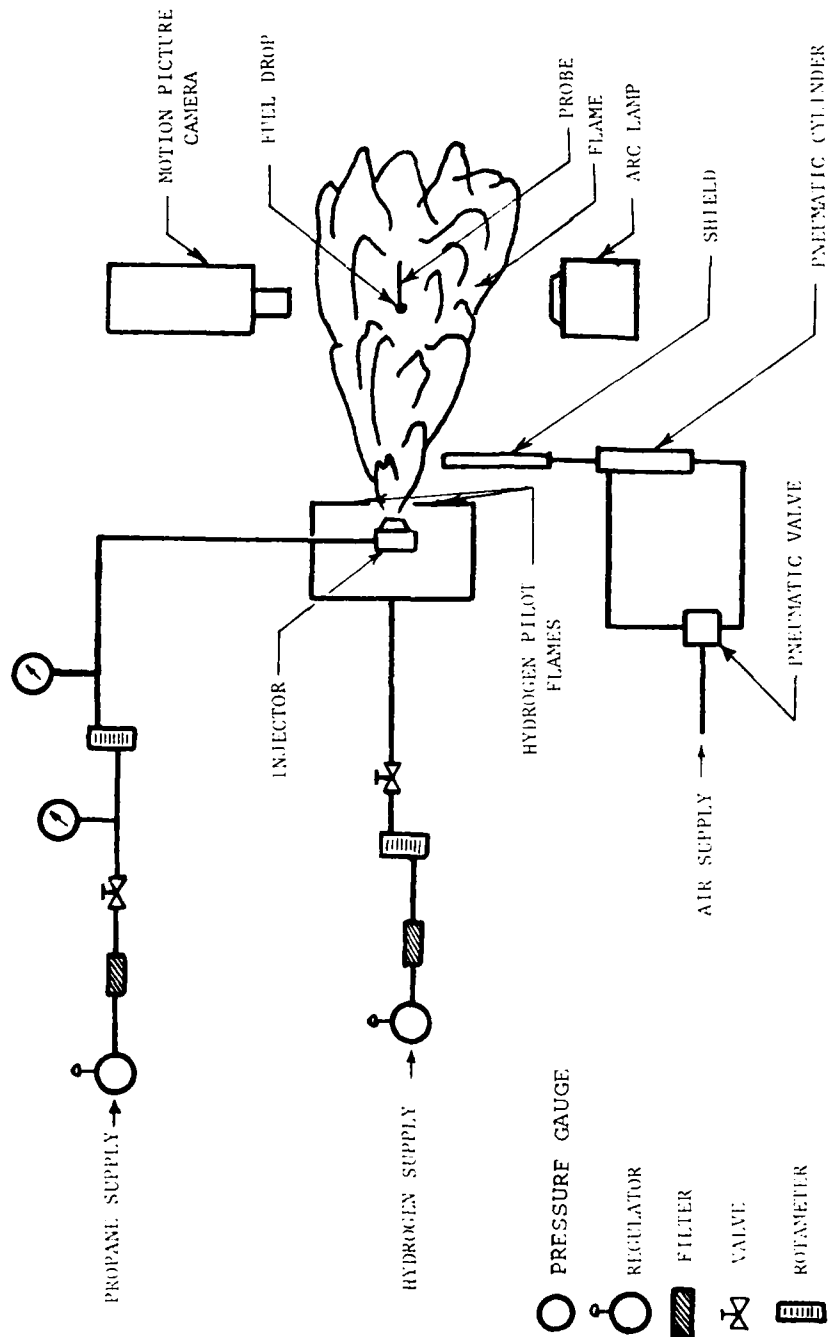


Figure 9. Test Apparatus Schematic.

The gas flame was stabilized near the exit of the injector using an array of four hydrogen capillary flames. The flame tubes were mounted in a symmetrically opposed pattern injecting toward the centerline of the injector passage. The flow passages for the hydrogen were slots 0.4-mm wide and 2.0-mm long, with the long axis parallel to the injector centerline. The lower edges of the slots were 1.8-mm above the face of the injector. The exit planes of the slots were 6.4-mm apart.

The propane gas flow rate was metered with a Matheson model 604 rotameter and controlled by a Harris model 25-15 pressure regulator with an output capacity of 0 to 0.69 MPa. The flow rate of the hydrogen gas was metered with a Matheson model 601 rotameter and controlled with a Matheson model 1H pressure regulator having a 0 to 1.38 MPa output capacity. The rotameters for both the propane and hydrogen flows were calibrated with a Precision Scientific Company wet-test meter (283 ml/rev).

The fuel droplets were mounted on quartz fibers with slightly enlarged ends to help support the drop. The fibers were mounted in turn on a metal bracket that extended into the flame.

The droplets were mounted on the fiber with a hypodermic needle. The flame was deflected from the mount region until the droplet was in place. The deflector was constructed from a 200 x 305-mm sheet of stainless steel, having a thickness of 3 mm. The droplet combustion process was initiated by removing the deflector with a pneumatic cylinder arrangement.

(2) Instrumentation

(a) Droplet Environment Measurements

The droplet environment at each test location within the flame was characterized. This involved measurements of mean velocity, temperature, and composition.

Velocities were measured with a single-channel laser Doppler anemometer (LDA). The instrument employs a Spectra Physics, model 125A, 50-mW helium-neon laser. The remaining components are manufactured by Thermo-Systems, Inc. The LDA was operated in the dual beam forward scatter mode. The sending and receiving optics had a focal length of 241 mm with an 11.6-degree angle between the beams. The aperture diameter of the photodetector was 0.256-mm. The signal was focused on the photodetector with a 200-mm lens. This produced an ellipsoidal measuring volume 3.0 mm in length with a diameter of 0.31 mm. A frequency shifter was used so that flow reversals could be detected. A bandpass light filter was used to limit the interference of the light from the flame. The signal from the photo-detector was processed using a frequency tracker in conjunction with an integrating digital voltmeter. Further details of this arrangement may be found in References 9 through 11.

The mean gas temperatures were measured using a thermocouple temperature probe manufactured from 50 μm diameter platinum/platinum-10-percent Rhodium wires, which were spot-welded onto 750 μm diameter lead wires of the same material. The fine wire thermocouples were manufactured by Omega Engineering, Inc. The radiation correction for this thermocouple was less than 35C over the test range. The reference junction was at the ambient temperature, shielded from the flame. An integrating digital voltmeter was used to average the signal over a two-minute time period.

Composition of the flame was measured by extracting gas samples from the flow at nearly isokinetic conditions using a water-cooled probe. The samples were analyzed with a Perkin Elmer Model 880 gas chromatograph using a hot-wire detector.

(b) Droplet Measurements

The droplet combustion process was observed with a 16-mm, Photosonics, Model 16-B motion picture camera. The camera optics provided a 2:1 magnification. The camera was powered with a Kepco, SM 36-5 AM dc power supply. The film speed was indicated with a timing light on the camera, activated with an Adtrol Electronic pulse generator, model 501. Kodak Plus-X reversal film was used for all tests.

Backlighting for shadowgraph measurements was provided by a Pek, Model 401A, 75-W mercury arc lamp. The light from the arc was collimated and directed toward the drop location. A diffuser screen was employed behind the drop to equalize the light intensity of the background. The background intensity was adjusted so that envelope flames around the drop could also be observed.

The film records were analyzed on a frame by frame basis, using a Vanguard motion picture analyzer. Photographs of objects of known size at the droplet location provided a calibration of particle size distances on the film.

Carbon residue left on the probe after combustion was examined with a scanning electron microscope (SEM), International Scientific Instruments, Model M-7. Permanent records of appearance of the residue were obtained with Polaroid film.

(3) Test Conditions

Initial tests with the slurries involved evaporation and combustion in room air. In this case, droplets were ignited by briefly exposing them to a flame. This provided a qualitative assessment of the ignition and sustained combustibility of the slurry samples with and without a combustion catalyst.

The bulk of the testing was undertaken at locations along the centerline of the gaseous propane diffusion flame. No external ignition source was employed for these tests. The burner operating conditions are summarized in Table 5. A photograph of the flame appears in Figure 10. A summary of mean velocities, temperatures and compositions in the flow is presented in Paragraph 2.c.(2). A complete analysis of this flame appears in References 9 through 12.

Initial drop sizes were in the range 500 to 5000 μm .

TABLE 5. BURNER FLAME CHARACTERISTICS.¹

Fuel:	Propane
Fuel flow rate:	176 mg/s
Initial fuel jet velocity:	88.7 m/s
Initial fuel jet diameter:	1.194 mm
Jet Reynolds number:	23600
Orientation:	Vertical (upward)
Flame Height:	460 mm (visual)
Injector Thrust:	15.6 mN
Hydrogen flow rate:	0.126 mg/s
Ambient and injector inlet temperature:	296 K
Ambient pressure:	97 kPa

¹Nozzle is Spray Systems Co. model 1/4J 2050 fluid nozzle and No. 67147 air nozzle, air atomizing injector.

12. C-P. Mao, G. A. Szekely, Jr. and G. M. Faeth, "Evaluation of a Locally Homogeneous Flow Model of Spray Combustion," to be published.

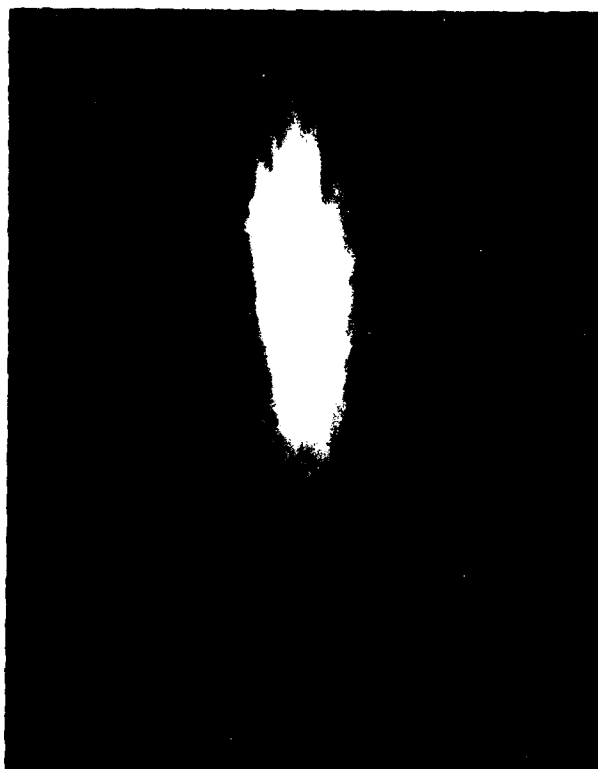


Figure 10. Photograph of the Turbulent Gas Diffusion Flame.

c. Fuel Droplet Experimental Results

(1) Droplet Processes in Air

(a) Observations

The pure JP-10 droplet burned in a conventional manner for a liquid fuel. An envelope flame was observed around the droplet until all the fuel was consumed. After an initial heat-up period, the square of the droplet diameter decreased in a linear fashion, which is typical behavior of supported droplets under natural convection conditions.

The initial phase of combustion of the noncatalyzed slurry droplets was similar to that of pure JP-10. An envelope flame was observed around the droplet and the droplet diameter decreased. This phase appeared to involve the combustion of the JP-10 in the slurry. However, after a time, the envelope flame was extinguished and a black residue remained on the probe. Although gravimetric measurements were not made, it appeared that most of the original solid carbon in the droplet remained unburned.

The catalyzed slurry droplets exhibited the most interesting combustion behavior in air. A typical dark field motion picture for this case appears in Figure 11. The early frames clearly show the envelope flame around the droplet persisting for nearly a second. After this flame extinguished little luminosity was present for a period of 2.8 seconds. Then the residue itself began to glow indicating reaction of the carbon. After a period of glowing (12.6 s, of which only the last 2.5 s are shown in the figure) the reaction extinguished again, leaving a carbon residue.

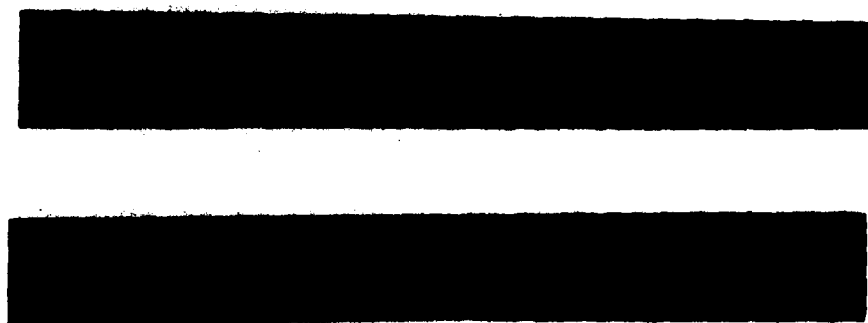


Figure 11. Dark Field Motion Picture Photographs
of a Catalyzed Slurry Droplet Burning
in Air.

The dark period prior to glowing probably involved reaction of the carbon, causing it to become heated. Glowing was observed where heating proceeded to a sufficiently high temperature so that the particle emitted significant radiation in the wavelength range for which the photographic system is sensitive. Thus, the absence of glowing is not necessarily indicative of no reaction, and even the uncatalyzed droplet may have undergone significant reaction.

These results clearly indicate that the catalyst has an important effect on the carbon reaction rate. By increasing the reactivity of the carbon, combustion can be sustained at higher rates in spite of heat losses to the surroundings, at least for a time. The slow step in the reaction process involves combustion of the carbon, which eventually will be the controlling step during spray combustion in a practical combustion chamber.

These observations indicate that the overall behavior of the present slurry droplets is qualitatively similar to the behavior observed for coal slurries (Ref. 3). In the present case, however, there was less disruption of the particles during combustion, probably due to the absence of the volatilization step for the solid.

Further insight concerning the slurry combustion mechanism was obtained by observing the residue with the SEM. As a baseline, Figure 12 is an illustration of the residue from a catalyzed slurry droplet, evaporated in air without combustion. In this case, the surface of the agglomerate is very smooth. This suggests that the particles in the slurry tend to pack together in a close array, with perhaps the smallest sized particles more prevalent at the surface.



Figure 12. SEM Photograph of Residue Following the Evaporation of a Catalyzed Slurry Drop in Air (Top X 50, Bottom X 200).

SEM photographs of the uncatalyzed slurry residue, after combustion in air, are illustrated in Figure 13. In this case, the residue appears smooth in some regions and rough in others. The residue also appears to be partly hollow. It was difficult to prevent some disturbance of the sample while it was transported and mounted in the SEM; therefore, the fractured zones may be due to handling problems. Certainly some areas are very similar to the appearance of the surface when no reaction occurred, e.g., Figure 12. The rough areas could be typical of the subsurface structure in cases of little reaction or could result from consumption of smaller particles.

Figure 14 is an illustration of SEM photographs of the residue of catalyzed slurry droplets following combustion in air. This structure is very different from the preceding cases. The residue has a more open structure and no smooth regions are observed. The reaction of the solid appears to extend a significant distance below the outermost surface of the particle. The smallest elements, observed at a magnification of 10,000, appear to have a characteristic diameter of approximately $0.3\text{ }\mu\text{m}$, which corresponds to the ultimate particle size of the slurry. These subelements are arranged in groups having a grape cluster appearance. The protuberance visible in the lower figure of Figure 14 (X 400) has a diameter of roughly $25\text{ }\mu\text{m}$, which would be more typical of the residue from a droplet produced under combustion chamber conditions. It is evident that particles of this size are irregular in shape and relatively porous.

(b) Burning Rates

Figure 15 is an illustration of the variation of droplet diameter as a function of time after ignition in air for the three fuels. The ordinate is the square of the droplet diameter,

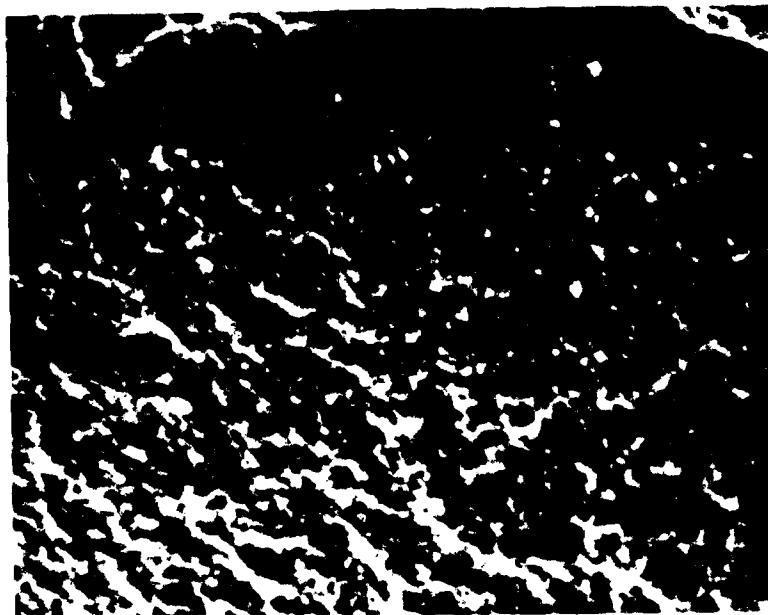


Figure 13. SEM Photograph of Residue Following the Combustion of a Noncatalyzed Slurry Drop in Air (Top X 50, Bottom X 400).

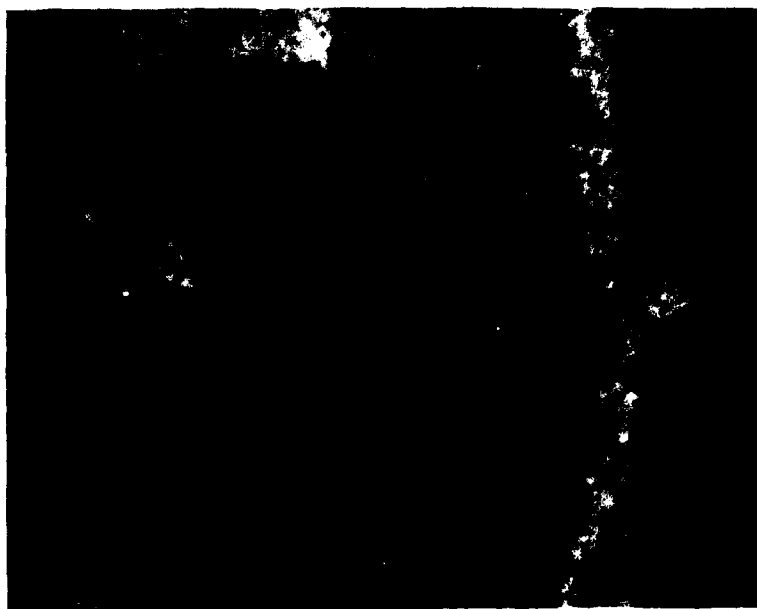


Figure 14. SEM Photograph of Residue Following the Combustion of a Catalyzed Slurry Drop in Air (Top X 100, Bottom X 400).

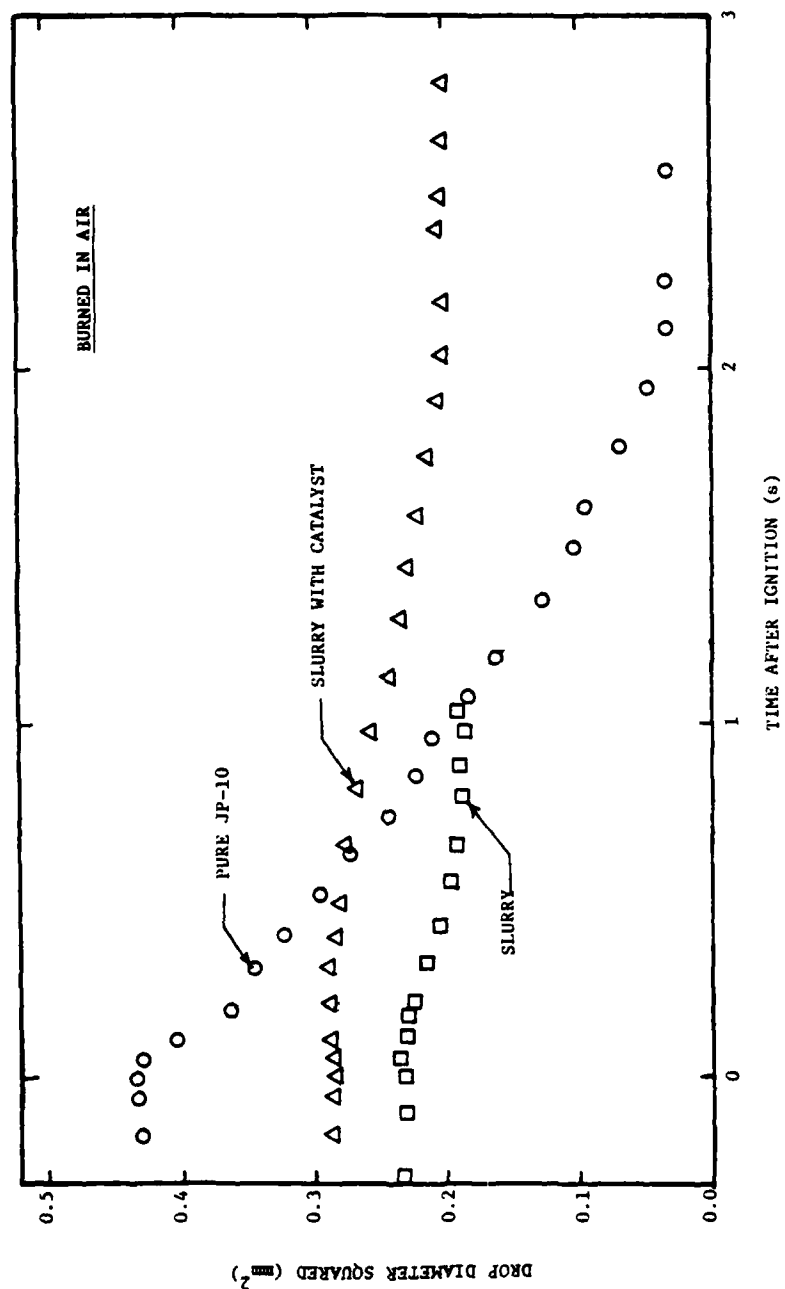


Figure 15. Droplet Diameter as a Function of Time for Three Fuels Burning in Air.

since the variation of this quantity with time is frequently linear for a pure liquid fuel droplet burning in still air (Ref. 13).

The particle diameters in Figure 15, typical of other data in this report, are the equivalent diameter of an ellipsoid having the same volume, e.g.

$$D = (D_{\min}^2 D_{\max})^{1/3}$$

where D is the reported diameter, and D_{\max} and D_{\min} are the major and minor diameters of the particle.

The slope of the diameter squared plot for JP-10 is nearly linear. Some variation of true linearity is expected since JP-10 is a blend, rather than a pure hydrocarbon. The enhancement of evaporation rates by natural convection also tends to decrease as the particle becomes smaller, causing some curvature in the plot.

The burning rate constant, K , is widely used to interpret droplet gasification rates. This parameter is defined as

$$-K = \frac{dD^2}{dt} \quad (2)$$

For JP-10, a mean burning rate constant of $0.2 \text{ mm}^2/\text{s}$ is obtained for the data illustrated in Figure 3-14. This is a typical value for hydrocarbon combustion in air.

The slurry droplets also exhibited a reduction in diameter in the region just after ignition, when an envelope flame was observed. As noted earlier, this is largely due to the combustion of JP-10. The apparent burning rate constant of the JP-10

13. G. M. Faeth, "Current Status of Droplet and Liquid Combustion," Prog. Energy Combust. Sci. 3, 191, 1979.

for the slurries, however, is less than the value obtained for the pure JP-10 droplet, roughly on the order of 0.05 to $0.1 \text{ mm}^2/\text{s}$. This type of behavior was not observed for droplets in the burner flame, where initial burning rates were similar for both pure JP-10 and the slurries.

Once the envelope flame extinguished, for the noncatalyzed slurry droplet, no further luminosity was observed, and the particle diameter remained constant. With catalyst present, however, the particle glowed after a dark period, and then extinguished again leaving residue. During the glowing period, however, there was relatively little variation in the diameter of the particle. This agrees with the SEM observations where the structure was rather porous following combustion of a catalyzed slurry droplet, suggesting reaction in depth rather than just at the surface. The bulk of the reaction in the glowing period is probably confined to the subsurface region where heat losses are reduced. As reaction proceeds, the structure becomes more porous while the outer portions remain in place. Final extinguishment then becomes a complex process related to heat losses, oxidant penetration into the pores of the structure, and perhaps loss of the catalyst.

(2) Droplet Processes in a Turbulent Flame

(a) Observations

Figure 16 is an illustration of the variation in mean properties along the centerline of the turbulent flame fueled with gaseous propane. In the region near the nozzle exit, gas velocities and the concentrations of propane are relatively high, while the temperature is low and oxygen is absent. Moving downstream, the gas velocity and concentration of propane decrease monotonically. The temperature increases at first, reaching a maximum at the flame tip where the fuel has disappeared and combustion

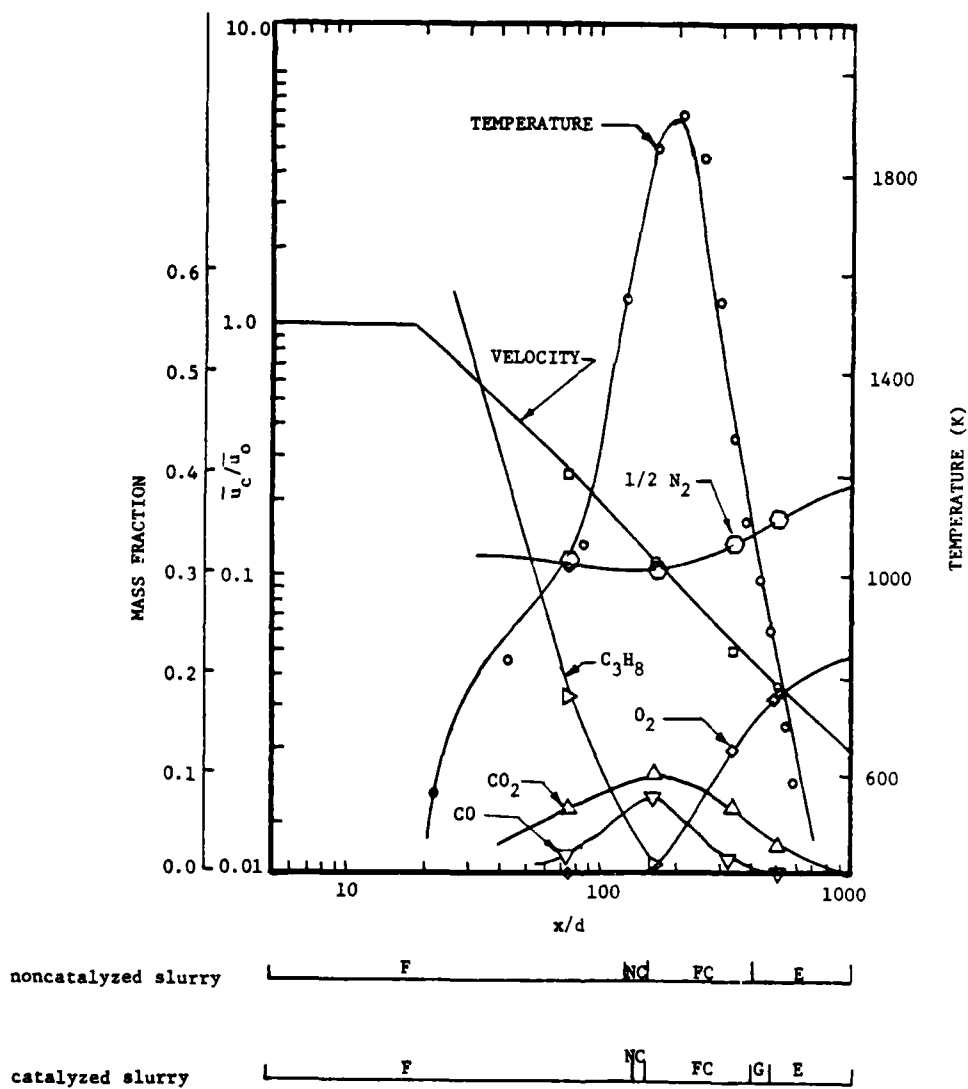


Figure 16. Flow Properties and Slurry Droplet Combustion Regions in the Turbulent Flame.

product concentrations are highest. Beyond the tip of the flame, the flow decays with increasing concentrations of oxygen and nitrogen and decreasing temperatures and combustion product concentrations.

The structure of the burner flame used in this study was typical of other gas and spray fueled diffusion flames (Refs. 9, and 12 through 14). The region near the injector was highly fuel rich and had a relatively low temperature. Significant concentrations of oxygen and high-temperature levels only appear as the turbulent reaction zone is approached.

Droplet behavior varied substantially with position in the flame. Table 3-6 is a description of the various types of behavior that were observed: fragmentation (F), noncombustion (NC), full combustion (FC), glowing (G), and evaporation (E). The regimes are listed in this order, which is the sequence they appear with increasing distance from the injector. Table 7 is a summary of the portion of the flame where the various regions were observed, for both the catalyzed and noncatalyzed slurries.

The various droplet burning regimes are also indicated on the lower part of Figure 16. The observations in each of these regions will be considered in turn.

Fragmentation Region. This region is closest to the injector, involving relatively high gas velocities and propane concentrations, moderate combustion product concentrations, virtually no oxygen, and temperatures from 300 to roughly 1600K. In this region, the liquid fuel evaporated with no envelope flame present. A luminous wake was visible behind the droplet as the

-
14. G. M. Faeth, "Spray Combustion Models -- A Review," AIAA Paper No. 79-0293, 1979.

TABLE 6. SUMMARY OF SLURRY DROP COMBUSTION REGIONS IN THE TURBULENT FLAME.

Region ¹	Designation	Description
Fragmentation	F	The liquid fuel evaporated without an envelope flame; however, a diffuse luminous wake was observed. When all the liquid was gone, some of the carbon agglomerate was fragmented into 3 to 5 large flakes. A carbon agglomerate also remained on the probe.
Noncombusting	NC	The liquid fuel evaporated without an envelope flame; however, a diffuse luminous wake was observed. When all the liquid had evaporated, a luminous wake of reduced intensity was still observed. A carbon agglomerate remained on the probe.
Full combustion	FC	An envelope flame was observed around the particle until the liquid fuel was consumed. After a dark period, the carbon agglomerate began to glow. Glowing continued until virtually all the carbon was consumed.
Glowing	G	The liquid fuel evaporated with no envelope flame observed. Some time after the liquid was gone (2 to 15 s for present test conditions), the carbon agglomerate began to glow. Glowing persisted until virtually all the carbon was consumed. This region was only observed for the catalyzed slurry.
Evaporation	E	The liquid fuel evaporated with no envelope flame observed. Glowing of the carbon agglomerate was not observed. No change of the particle size was observed once the liquid was gone for the noncatalyzed slurry. Some reaction of the catalyzed slurry was observed in the upstream end of this zone.

¹In order of increasing distance from the injector.

TABLE 7. SUMMARY OF SLURRY DROP COMBUSTION REGIONS IN THE TURBULENT FLAME

Region	Designation	Range x/d^1	
		Catalyzed Slurry	Noncatalyzed Slurry
Fragmentation	F	$42^2 - 138$	$42^2 - 128$
Noncombusting	NC	$143 - 154$	$132 - 154$
Full Combustion	FC	$159 - 404$	$159 - 383$
Glowing	G	$409 - 500$	--
Evaporation	E	$505 - 680^3$	$404 - 680^3$

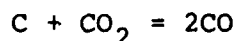
¹Gaps in the ranges are due to finite spacing of test locations.

²Nearest point to injector considered. There was no evidence that closer locations would not be in the fragmentation region.

³Farthest point from the injector considered. There was no evidence that locations farther downstream would not be in the evaporation region.

liquid evaporated. This behavior is typical of a liquid fuel evaporating in a high-temperature gas in the absence of oxygen (Refs. 13 and 15). The liquid droplet primarily evaporated without combustion. As the fuel gases became heated, they decomposed forming soot. When the temperature was high enough, the soot glowed yielding a diffuse luminous wake.

When the bulk of the liquid had evaporated, most of the carbon agglomerate was blown off the probe in three to five large flakes. The mechanical breakdown of the agglomerate resulted from the relatively high gas velocities in this region. Figure 17 is a SEM photograph of the residue remaining on the probe after exposure of a catalyzed slurry droplet to the fragmentation region of the flame. The appearance of the residue from the non-catalyzed slurry was similar. The surface is very irregular with waves frozen into the structure by the high gas velocity. The surface structure is similar to that observed when these droplets were burned in air, see Figure 14. At higher magnifications, subelements having a size comparable to the ultimate carbon particle size, $0.3 \mu\text{m}$, were observed. Some oxidation of the surface cannot be precluded, particularly near the downstream end of this zone. The mechanism of residue reaction in this region would involve oxidation of carbon by carbon dioxide



since oxygen concentrations are low. Oxidation is clearly not complete, however, many carbon particles are transported downstream for subsequent oxidation in regions of the flame that have higher temperature and oxygen levels (similar to the burnout of soot formed in the cool core of a turbulent flame).

-
15. G. M. Faeth and R. S. Lazar, "Fuel Droplet Burning Rates in a Combustion Gas Environment," AIAA J 9, 2165, 1971.

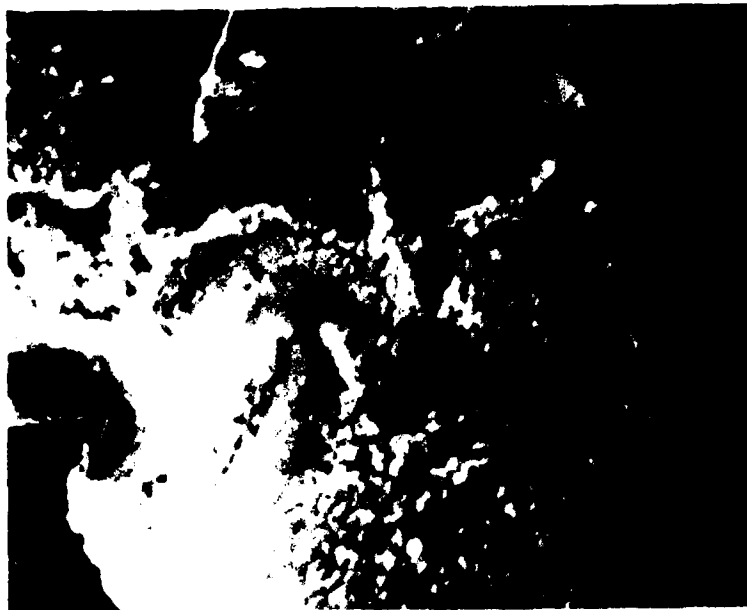


Figure 17. SEM Photograph of Residue from a Catalyzed Slurry Drop in the Fragmentation Region, $x/d = 75$ (Top X 150, Bottom X 5000).

Noncombusting Region. This region was relatively narrow for both fuels. It was located on the fuel-rich side of the reaction zone. Here, velocities and oxygen concentrations were relatively low, while temperatures and product concentrations approach their maximum values. The liquid fuel evaporated without an envelope flame, similar to behavior in the fragmentation region. There was little flaking of the residue, however, and greater amounts of carbon remained on the probe. After the liquid had evaporated, a luminous wake of reduced intensity was still observed. This suggests continued shedding of small carbon particles that eventually glowed as they heated (and began to react) in the flow.

Figure 18 is a SEM photograph of the surface of the residue in this region. The residues from both noncatalyzed and catalyzed slurries were similar. The structure is similar to the structure seen in the fragmentation region. The major difference between the two regimes is that the lower velocities did not cause the residue to flake. Rates of reaction from carbon dioxide were also probably somewhat higher although the rates were still relatively low. As the CO_2 attacked the structure, the support of particles was weakened, probably causing small units to flake off for an extended period of time.

Full Combustion Region. The full combustion region had low gas velocities, and relatively high temperatures and high concentrations of oxygen and combustion products. An envelope flame was observed around the droplet as the liquid evaporated. Similar to combustion in air, a dark period was observed between the time when the envelope flame was extinguished and the residue began to glow. The dark period involved transient heating of the surface from the low-temperature levels characteristic of liquid evaporation to the high temperatures characteristic of carbon reaction. In contrast to combustion in air, both the noncatalyzed and catalyzed slurry residues exhibited glowing in the



Figure 18. SEM Photograph of the Residue from a Catalyzed Slurry Drop in the Noncombusting Region, $x/d = 149$ (X 5000).

burner flame. The glowing persisted until very little carbon residue remained.

Figure 19 shows SEM photographs of the residue from a catalyzed slurry droplet in this region. The residue from the non-catalyzed slurry was similar. The structure is thin and very porous. In this region, the residue was a cenosphere. This behavior was probably the result of convective and radiative heat losses, which tended to quench the reaction at the outer surface. The shielding effect of the outer structure allowed higher temperature levels below the surface of residue, and the reaction completed the gasification of the solid within the interior of the particle. The greater extent of reaction near the outer surface resulted in a structure that was less related to the original slurry particles than was the case for the region nearer to the injector.

Glowing Region. This region was only observed for the catalyzed slurry, and was relatively narrow. Oxygen concentrations were relatively high in this region (mass fractions in the range 0.15 to 0.20) and temperatures were relatively low (800 to 1000K). The liquid fuel evaporated with no envelope flame present and no luminous wake. Some time after the liquid was gone, 2 to 15 s for present test conditions, the residue began to glow. Glowing persisted until little carbon was left on the probe.

The surface structure of the residue from this region was similar to the full combustion region. SEM photographs of the surface appear in Figure 20. The structure is very porous.

Evaporation Region. The evaporation region was farthest from the injector, where the flow decays to approach the properties of room air. In this region, the liquid evaporated leaving a carbon agglomerate. There was little evidence of subsequent reaction of the agglomerate.



Figure 19. SEM Photographs of Residue from a Catalyzed Slurry Drop in the Full Combustion Region, $x/d = 340$ (Top X 100, Bottom X 5000).

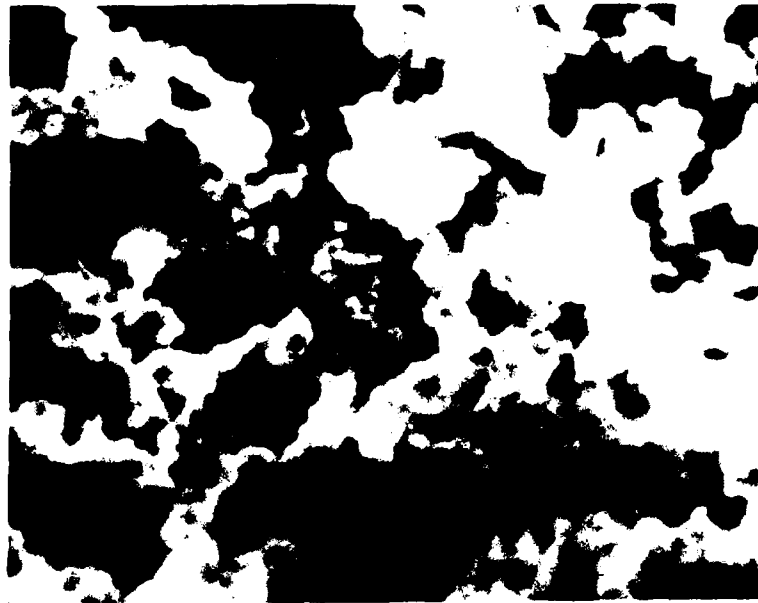


Figure 20. SEM Photographs of Residue from a Catalyzed Slurry Drop in the Glowing Region, $x/d = 489$ (Top X 2000, Bottom X 5000).

SEM photographs of the residue in this region appear in Figure 21. The surface appears smooth in some regions and coarse in others (due to fracture of the sample). The appearance is generally similar to evaporation in air with little reaction of the agglomerate, see Figures 12 and 13.

Effect of Catalyst. The appearance of the residue from both slurry fuels was similar in each region. The main effect of the catalyst was to extend the region where reaction of the residue could be sustained. For example, the noncatalyzed residue reacted in the range $x/d = 159$ to 383 , while the catalyzed residue reacted in the range $x/d = 159$ to 500 . This substantially increases the residence time where reaction of residue occurs in the flow. For example, if the particles are small enough to move with the gas velocity, then:

$$t_r = \int_{x_i}^{x_e} dx/u \quad (3)$$

where x_i and x_e are the beginning and end of the reaction region, t_r is the residence time in the reaction zone, x is distance from the injector, and u is the gas velocity. Completing the integration of Eq. (3) for present burner conditions yields $t_r = 41$ ms for the noncatalyzed residue and $t_r = 76$ ms for the catalyzed slurry -- almost twice as long. Naturally, within an actual combustion chamber, conditions will be different. It seems likely, however, that the catalyzed slurry residue will react over a greater portion of the flow.

(b) Burning Rates

Data on the variation of droplet diameter as a function of time are examined in the following paragraphs. The three main

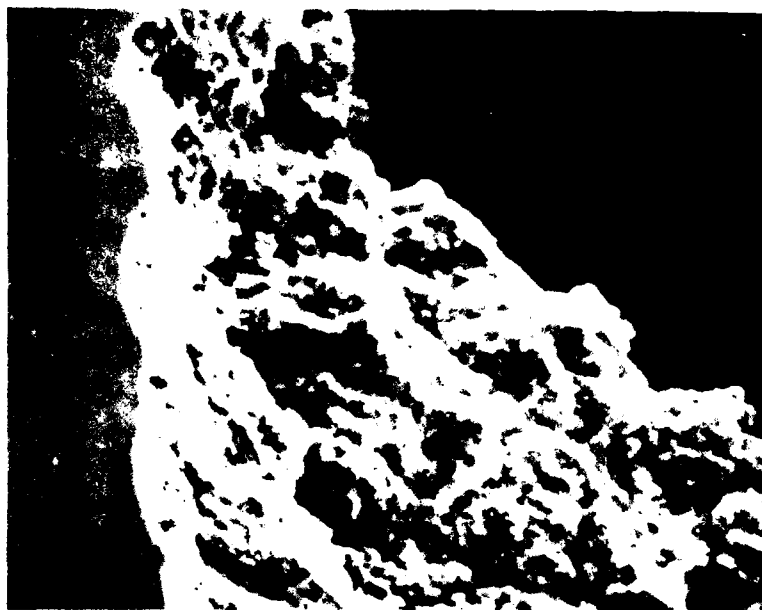


Figure 21. SEM Photographs of Residue from a Catalyzed Slurry Drop in the Evaporation Region, $x/d = 510$ (Top X 4000, Bottom X 3000).

combustion regimes are considered: the fragmentation region, $x/d = 75$; the full combustion region, $x/d = 340$; and the evaporation region, $x/d = 510$. The flow properties at each of these locations are summarized in Table 8.

Fragmentation Region. Figure 22 is an illustration of the variation of droplet diameter, as a function of time, for the three fuels in the fragmentation region. The square of the droplet diameter is plotted so that the results can be associated with burning or evaporation rates.

The evaporation-rate constant of pure JP-10 was roughly $1 \text{ mm}^2/\text{s}$ at this location, compared to $0.2 \text{ mm}^2/\text{s}$ for combustion in still air (see Figure 15). The increase occurred in spite of the fact that the fuel evaporated with no envelope flame present. The reason for this was the relatively high gas velocity at the test location, which increased convection effects.

The evaporation constants of the two slurry droplets were similar to that of pure JP-10, in the early stages of evaporation. As the liquid disappeared, however, the rate of reduction of the particle size was reduced, due to the presence of the solid. Continued drying of the slurry, after a delay period, weakened the structure of the slurry. This caused flaking off of large particles (3 to 5 flakes) and an abrupt reduction of the diameter of the residue. The residue that remained was similar for both the noncatalyzed and catalyzed slurries, see Figure 17.

Full Combustion Region. Figure 23 is an illustration of the variation of particle diameter with time for the three fuels in the full combustion region. The evaporation constants of the three fuels were similar in the initial stages of the process where evaporation of JP-10 dominates (1.1 to $1.2 \text{ mm}^2/\text{s}$). The fact that this rate was nearly the same as in the blow-off region at $x/d = 75$ is fortuitous. The higher oxygen concentration and

TABLE 8. SUMMARY OF FLOW PROPERTIES AT SELECTED DROP LOCATIONS.

	x/d		
	75	340	510
Gas velocity (m/s)	26.6	4.6	3.1
Gas temperature (K)	998	1193	720
Gas composition (mass fraction)			
N ₂	0.57	0.72	0.75
O ₂	0.00	0.12	0.18
CO	0.20	0.00	0.00
CO ₂	0.05	0.08	0.04
H ₂ O	0.04	0.04	0.02
H ₂	0.03	0.00	0.00
C ₃ H ₈	0.16	0.00	0.00
SEM photograph	Fig. 3-16	Fig. 3-18	Fig. 3-20
JP-10 evaporation rate constant (mm ² /s) ¹	1.0	1.1 - 1.2	0.6
Slurry residue burning rate constant (mm ² /s) ²	0.0	0.45 - 0.50	0.15

¹Essentially the same for all three fuels.

²Residue from catalyzed slurry only.

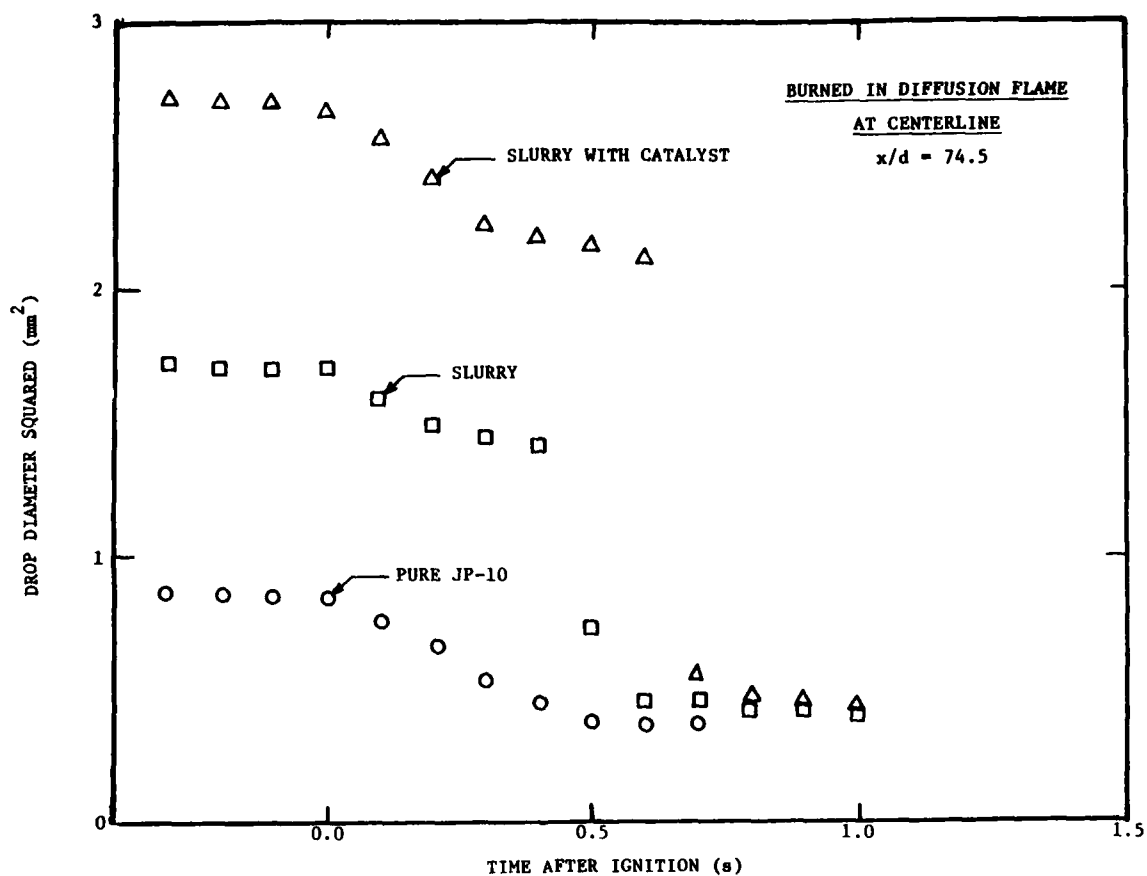


Figure 22. Droplet Diameter Variation as a Function of Time for the Three Fuels in the Fragmentation Region, $x/d = 75$.

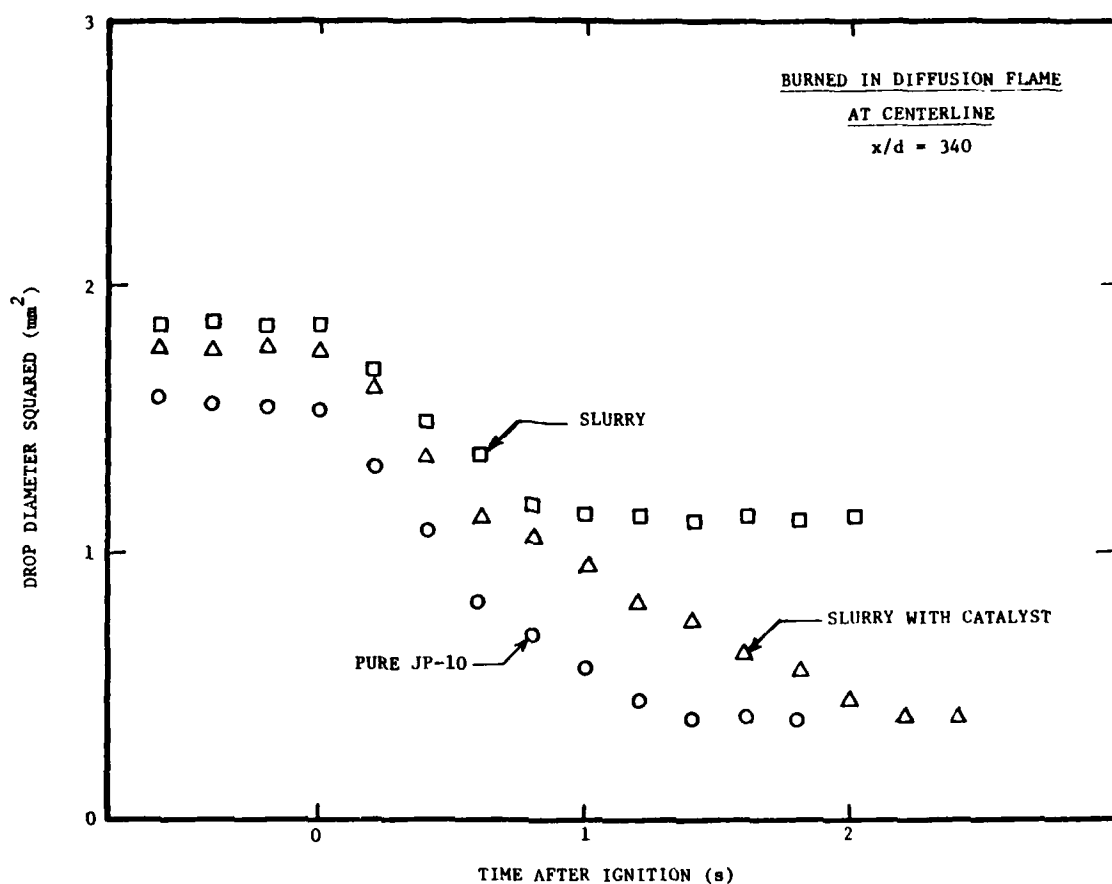


Figure 23. Droplet Diameter Variation as a Function of Time for the Three Fuels in the Full Combustion Region, $x/d \approx 340$.

ambient temperature at $x/d = 340$ were partly compensated by the lower gas velocity.

The noncatalyzed slurry exhibited a glowing period but was quenched before the residue was completely consumed. In contrast, the residue from the catalyzed slurry was almost completely consumed. As noted earlier, the residue of both slurries was similar.

Since the reaction of the residue was not limited to the surface, a burning rate constant has less meaning. However, an apparent burning rate constant for the catalyzed slurry of 0.45 to 0.50 mm^2/s can be obtained for the data illustrated in Figure 23.

Evaporation Region. Figure 24 is an illustration of the variation of particle diameter with time for the three fuels in the evaporation region. Similar to the other regions, the evaporation rate constant of the three fuels was similar in the region where JP-10 gasification dominates. A value of 0.6 mm^2/s can be extracted from the data.

Once the evaporation of JP-10 was complete, the noncatalyzed slurry exhibited little further reaction. In contrast, even though glowing was not observed, the diameter of the catalyzed slurry particle continued to decrease. The apparent burning rate constant of the slurry is 0.15 mm^2/s for the data illustrated in Figure 24. Thus, the absence of glowing did not preclude additional reaction of the residue. It should be noted, however, that the test location of Figure 23 was close to the end of the full combustion region ($x/d = 500$). Further downstream, much less reaction of the catalyzed slurry was observed.

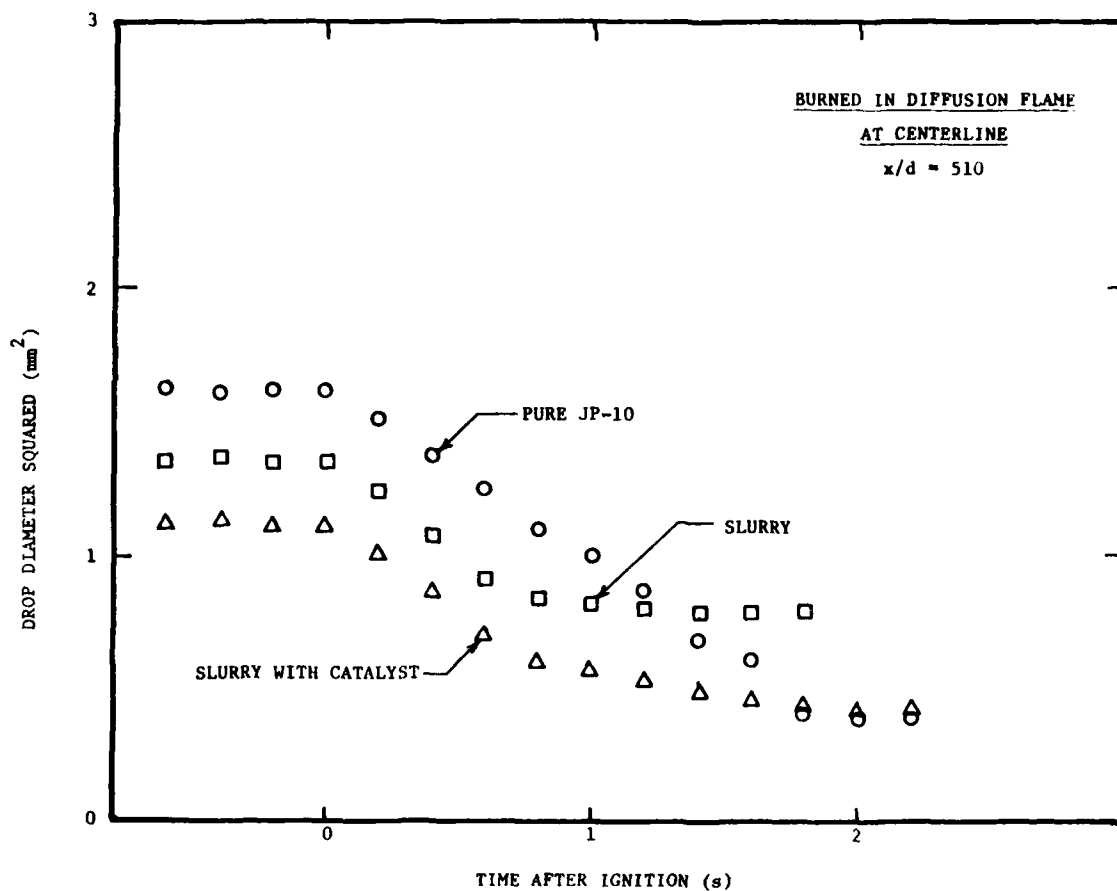


Figure 24. Droplet Diameter Variation as a Function of Time for the Three Fuels in the Evaporation Region, $x/d = 510$.

d. Conclusions

The tests reported herein involved supported droplets in the diameter range 500 to 5000 μm , placed in a turbulent flame at atmospheric pressure. The flame was produced by a propane jet issuing into stagnant room air. The radiant environment of the flame was optically thin.

While the test environment simulated some aspects of combustion chamber conditions, there were important differences. The test droplets were much larger than those encountered during normal combustion operation. Radiant losses from the particles during these tests were higher than would be encountered in a combustor, where flame radiation is more significant due to higher pressure levels, and the process is surrounded by heated surfaces. Finally, the region far from the injector approached stagnant room air during the present tests, rather than turbine inlet conditions for a combustor. These differences should be kept in mind as the conclusions of the present tests are considered.

The major conclusions of the present experimental investigation can be summarized as follows:

- (a) The life history of a carbon-slurry droplet can be broken down into four major stages:
 - (1) Heat up of the particle to temperature levels appropriate for evaporation of the liquid. Possible ignition of liquid fuel vapors.
 - (2) Evaporation, and possibly combustion, of the liquid fuel in a relatively conventional manner accompanied by agglomeration of the carbon particles into a solid residue.

- (3) Further heating of the carbon residue once all the liquid has evaporated.
 - (4) Ignition, or a gradually increasing reaction rate of the carbon, followed by combustion of the residue.
- (b) The behavior of the particles varied significantly throughout the flame. The various combustion regimes are identified in Table 6. They are characterized by the presence or absence of envelope flames, residue reaction, and residue breakup.
- (c) Combustion of the carbon residue was slow in comparison to the gasification of the liquid and is probably the controlling step during combustor operation. While evaporation of the liquid can occur everywhere in the flame, reaction of the carbon residue is limited to high-temperature regions where oxygen is present. In view of this behavior, it is probably desirable to delay dilution in combustors burning slurries (similar to pulverized coal furnaces) in order to provide more time for oxidation of the residue and to reduce premature quenching.
- (d) The carbon residue broke up into smaller fragments in the high relative velocity region near the injector. Otherwise, most of the carbon formed a single residue particle whose size was controlled by the initial drop-let size. In this circumstance, the desirability of fine atomization for practical combustors is obvious.
- (e) Addition of the catalyst significantly increased the size of the region of the flame where reaction of the

residue occurred. Catalyzed slurry residue also reacted more completely.

(f) Following active carbon combustion, the residue had an open lacey structure indicating that reaction was occurring to some depth in the particle. The subelements of this structure were approximately the same size as the ultimate particle size in the carbon black ($0.3 \mu\text{m}$).

(g) Cenospheres were observed as carbon residue in some cases. It is postulated that they resulted from quenching of the reaction at the outer surface of the particle, due to excessive radiative and convective heat losses to the environment.

3. Combustion Evaluation of Slurry-Fuel Samples

a. Combustion Evaluation Background

The combustion evaluation of the fuel samples supplied by Suntech was conducted by AiResearch. This evaluation consisted of atmospheric-combustion rig testing, pressure-combustion rig testing and engine testing. All testing was conducted on single-fuel-injector can combustors because of their simplicity, economy of operation, and availability. Results obtained from this testing will serve as the basis for progressing to annular combustor configurations in the future.

The atmospheric rig permitted qualitative assessments to be made through visualization of the exhaust flame from the combustor. Results obtained from these tests were used to define necessary combustor modifications for the demonstrator engine combustor and in the selection of the best available fuel formulation within the time constraints of the program. The pressure

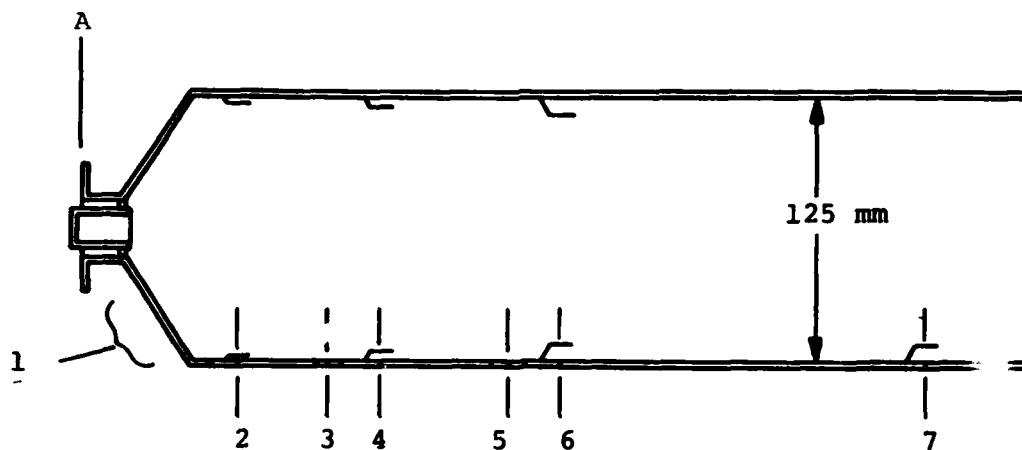
rig tests were conducted with the combustion system from the demonstrator engine and yielded quantitative data on the performance and operation of the combustor with both a baseline JP-4 fuel and the selected carbon-slurry formulation. The engine testing, conducted on a ETJ131 turbocharger/turbojet, provided a demonstration of the operation of an engine on carbon slurry for approximately a half-hour of operation.

The results from the testing provided preliminary design criteria for progressing to an annular combustor that would be capable of operation on carbon-slurry fuel. It also provided the basis for upgrading future fuel formulations consistent with ultimate specification goals while remaining feasible for turbine engine operation.

b. Atmospheric Testing

The first atmospheric flame visualization test was conducted in an existing 125-mm diameter can combustor as shown in Figure 25. The primary and dilution orifices were located 90.9 and 172.1 mm, respectively, downstream from the nozzle face. The three cooling orifices were located at 43.7, 115.2 and 199 mm, respectively. The primary recirculation zone was established by dome louvers (Row No. 1) and primary orifices (Row No. 3). Earlier spray and nozzle contamination tests had indicated that conventional filming airblast or pressure atomizing nozzles would be unsuitable for injecting carbon slurry due to clogging problems. Therefore, a low-cost AiResearch fuel nozzle with a single fuel delivery tube was used in all of the atmospheric tests. The rig used for all the atmospheric testing is shown installed in the test facility in Figure 26.

The first series of tests were conducted at a low combustor-inlet temperature of approximately 366K with a liner pressure drop equal to 3.0 percent. The corresponding combustor airflow



Row No.	Type Orifice	No. of Orifices	Orifice Diameter mm	Distance From A mm	Total Area mm ²	Airflow Percent Total
1	Cooling	30	3.58	37.34	301.98	7.68
2	Cooling	30	4.42	64.26	460.23	11.70
3	Primary	6	11.18	111.0	589.01	14.97
4	Cooling	30	4.80	135.76	542.87	13.80
5	Dilution	6	14.22	192.13	952.88	24.22
6	Cooling	30	4.80	219.58	542.87	13.8
7	Cooling	30	4.80	310.39	542.87	13.8

NOTE: Fuel Nozzle Area = 167.11 mm²
Percent Total Airflow = 4.25

Figure 25. Baseline Combustor Configuration and Airflow Distribution.

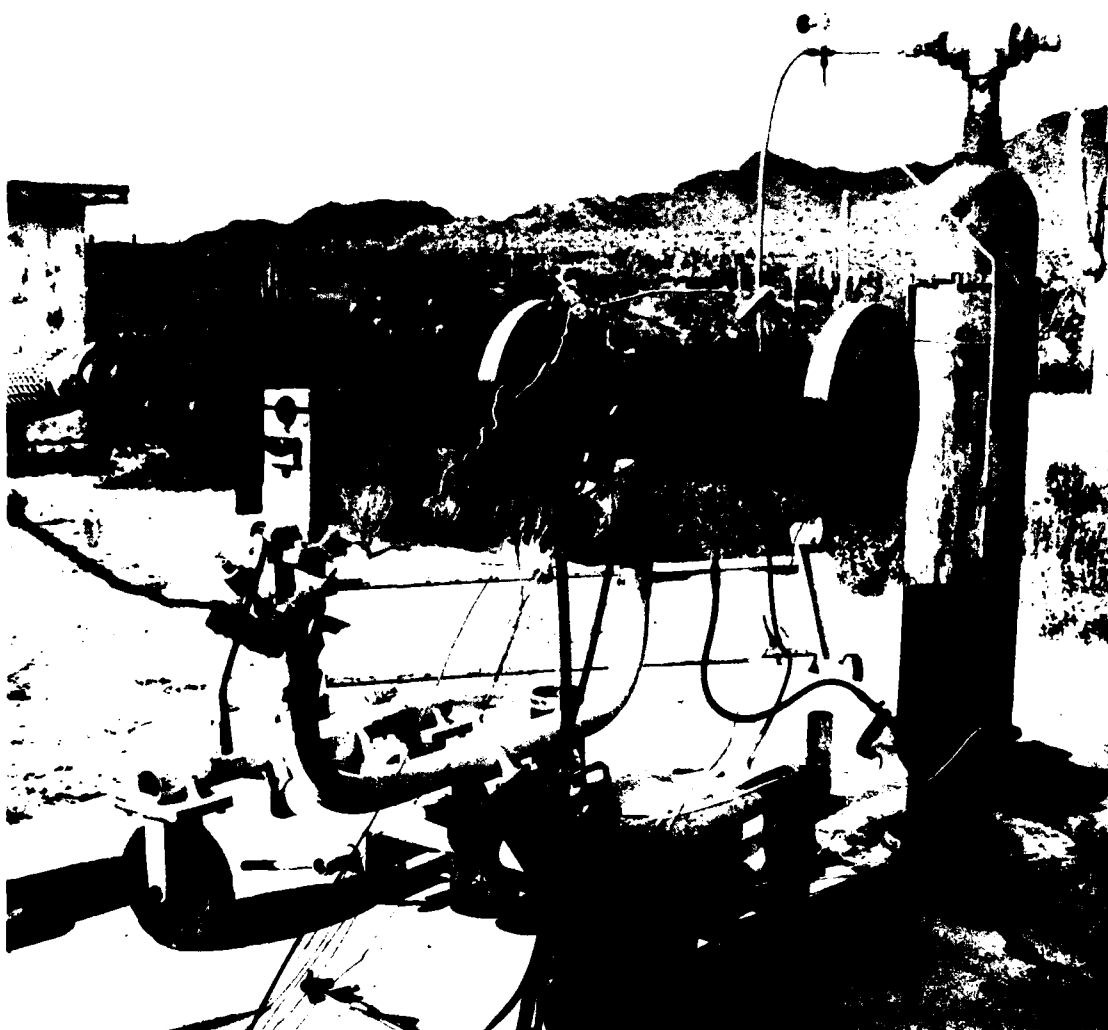


Figure 26. Atmospheric Combustor Test Rig.

rate was 0.161 Kg/s. The combustor reference velocity, residence time up to dilution orifices, and air loading parameter ($\phi = W_a / \delta^{1.7} V_e T / 540$) were 14 m/s 11.7 ms and 24.2 Kg/s M³, respectively. The rig was ignited and stabilized on JP-4 prior to switch over to carbon-slurry fuel which was supplied from a bladder delivery system.

A JP-4-fueled flame was first stabilized at an overall fuel/air ratio of 0.024 before switching to carbon slurry without catalyst (Suntech Sample 790-928). However, the flame did not remain ignited with carbon slurry even though the primary zone fuel/air ratio was 0.158. The corresponding fuel/air ratio based upon the JP-10 contents of 49.6 percent was 0.0785 or an equivalence ratio of 1.16. This indicated that in order to successfully burn carbon-slurry fuel a higher combustor inlet temperature was needed. It was also desirable to maintain high gas temperatures near the liner walls to help burn carbon particles that escaped the primary-zone hot-gas core. A carbon buildup on the combustor liner surfaces was noted following the test without a catalyst. The presence of a catalyst to enhance combustion or to lower carbon particle ignition temperature was considered to be necessary.

The second series of tests were conducted at different combustor inlet temperatures. In addition, the primary-zone-liner cooling air was reduced by blocking every other orifice of the dome louvers (Row No. 1) and the first cooling slot (Row No. 2), as indicated in Figure 27. Surface thermocouples were placed at five different axial stations to monitor wall temperatures in order to qualitatively correlate wall temperature levels with unburned carbon emitted by the combustor. The measured wall temperatures at different combustor inlet temperatures with the JP-4 fuel are presented in Figure 28 for the five axial stations. The corresponding data with the carbon slurry were not taken due to the limited quantity of the available fuel that did not allow sufficient time for recording the data.



Row No.	Type Orifice	No. of Orifices	Orifice Diameter mm	Distance from A mm	Total Area mm ²	Airflow Percent Total
1	Cooling	15	3.58	37.34	150.99	5.73
2	Cooling	15	4.42	64.26	230.11	8.74
3	Primary	6	11.18	111.0	589.01	23.37
4	Cooling	15	4.80	135.76	271.43	10.31
5	Dilution	6	14.22	192.13	952.88	36.19
6	Cooling	15	4.80	219.58	271.43	10.31

NOTE: Fuel Nozzle Area = 167.11 mm²
Percent Total Airflow = 6.35

Figure 27. Baseline Combustor with Reduced Primary Zone Cooling Air.

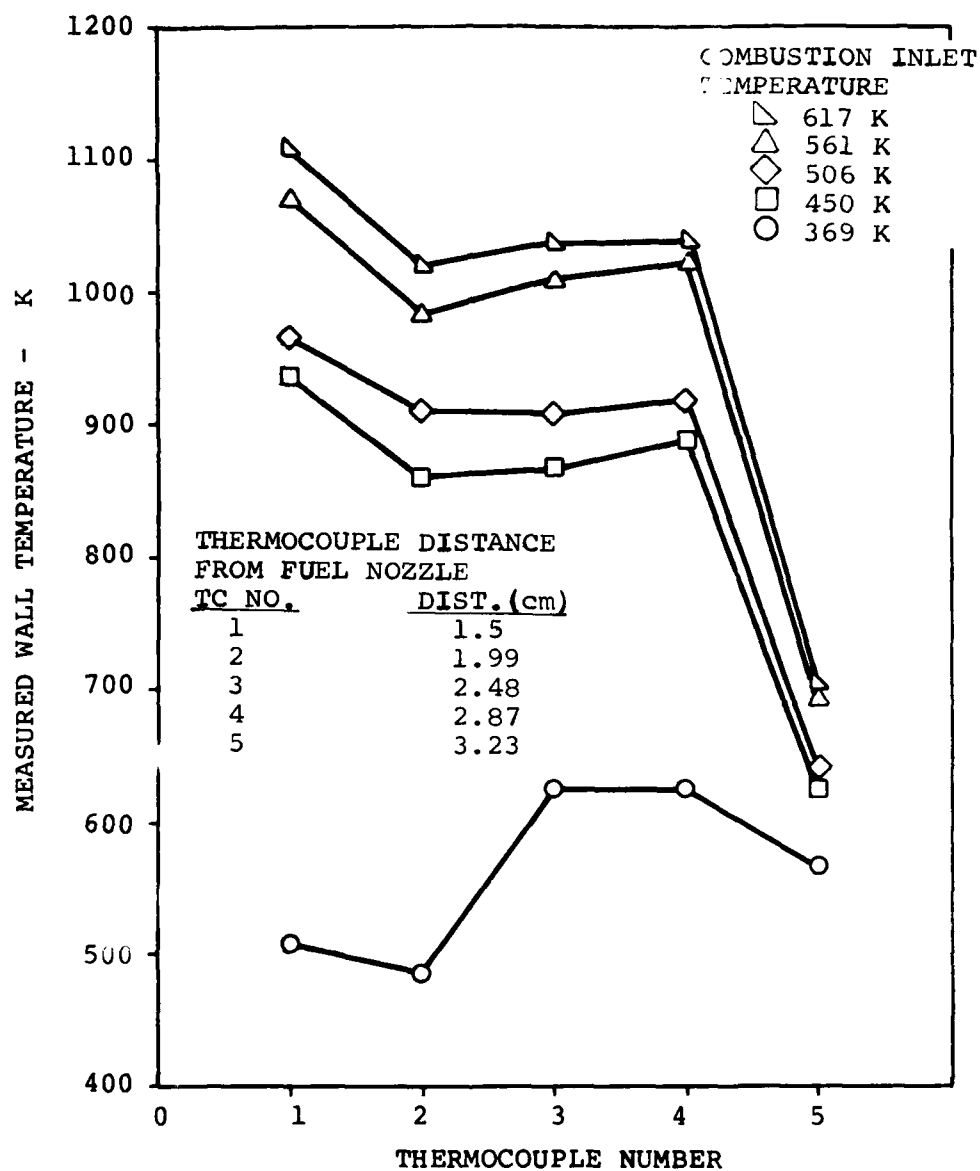


Figure 28. Measured Wall Temperature Using JP-4 Fuel.

When tested with the carbon-slurry fuel without catalyst, the smoke emitted at a $T_3 = 617\text{K}$ was excessively high. This indicated the desirability of using a catalyst even with high liner wall-temperature levels. Alternatively, it is anticipated that new combustion concepts must be evaluated wherein enhanced primary zone and intermediate zone residence times are possible. However, time constraints did not permit this to be done.

The reduced cooling-air conventional-combustor configuration (Figure 27) was subsequently tested with carbon-slurry fuel containing a lead catalyst with the carbon. With the addition of the catalyst (Suntech Sample 790-969), it was possible to sustain combustion at $T_3 = 450\text{K}$, although the amount of carbon emitted was excessively high. In addition, the flame was not contained within the combustor can. However, as the combustor inlet temperature was increased to 617K the flame length was reduced in addition to achieving a reduction in the smoke levels. At 617K , the flame barely extended beyond the combustor exit and emitted only small amounts of smoke. Liner carbon fouling was not observed. The conclusions reached from this test were as follows:

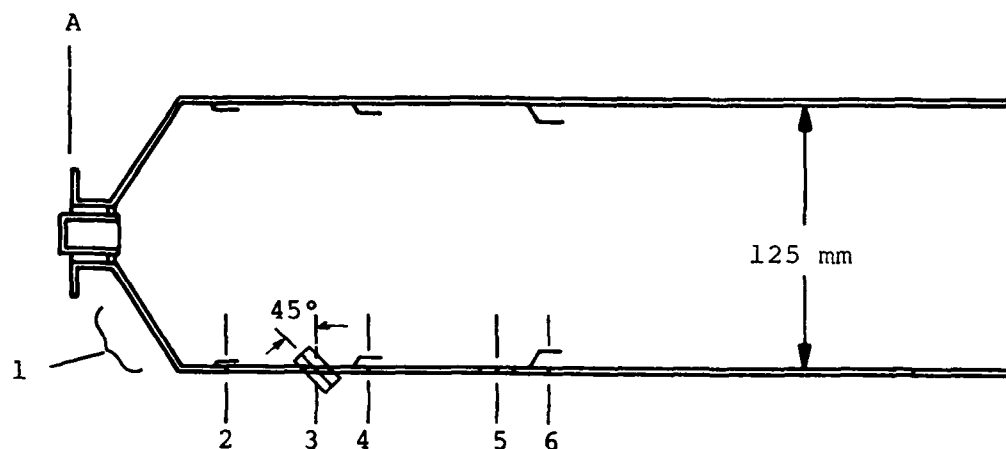
- o Carbon slurry with a lead catalyst can be burned successfully in a dome-louver stabilized can combustor at high inlet temperature levels of 617K or higher.
- o Exhaust smoke was low and no carbon fouling was observed.
- o New combustor concepts are needed for burning carbon slurry at low inlet temperatures (around 450K).

In order to improve the primary zone recirculation pattern so as to aid in the ignition of carbon particles, the baseline combustor primary orifices (Figure 27) were replaced by tubes that directed air toward the dome with a 45-degree angle, as

shown in Figure 29. The tube axial location was not changed from the baseline primary orifice location because of time constraints. The flame with JP-4 fuel was in six distinct quadrants as influenced by the six dome louvers. In addition, the flame pockets kept jumping from one quadrant to another. It was hypothesized that either the tubes were located too close to the dome or the amount of air flowing through the tubes was excessive, leading to pulsation. Consequently, the tube inlet area was reduced by 50 percent by brazing washers at the inlet. The resulting combustor (Figure 30) gave a stable flame with the JP-4 fuel. However, with carbon slurry, the flame did not stay ignited at $T_3 = 450K$ and $F/A = 0.024$. As the burner fuel/air ratio was increased, it was possible to sustain combustion, but excessive smoke was produced even at a $F/A = 0.04$. This indicated that more primary residence time was needed, which led to a Mod IIIA combustor as shown in Figure 31.

The Mod IIIA combustor was similar to the Mod IIA except for the location of the primary tubes. In order to afford a long carbon burn-out time, the dilution orifices were blocked. This resulted in the flame extending beyond the combustor exit plane. But it was hypothesized that if dilution orifices were installed, the flame would become contained within the can. The Mod IIIA configuration gave a marginally stable flame at $T_3 = 450K$ and $F/A = 0.033$; i.e., the flame would blow out occasionally. However, a stable flame with small levels of smoke was achieved at $F/A = 0.049$. The flame was extending beyond the can exit. As the fuel/air ratio was increased to 0.0756, the flame was larger and the smoke level was less.

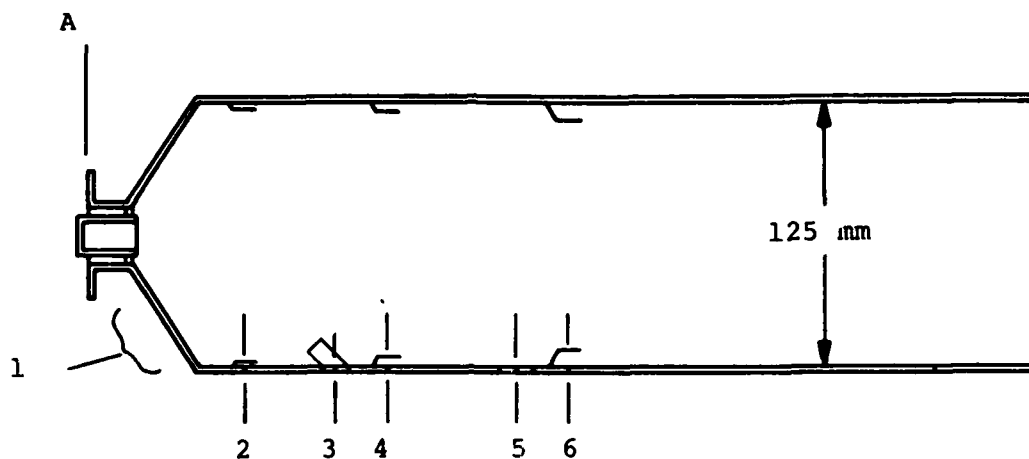
In order to reduce exhaust smoke, the Mod IIIB combustor (Figure 32) without dilution orifices was tested. This combustor was similar to the Mod IIIA except primary tube air was reduced as shown. This combustor was also marginally stable like Mod IIIA at $T_3 = 450K$ and $F/A = 0.024$. However, the exhaust smoke at $F/A = 0.048$ was negligible. At a still higher fuel/air ratio



Row No.	Type Orifice	Number of Orifices	Orifice Diameter mm	Distance from A mm	Total Area mm ²	Airflow Percent Total
1	Cooling	15	3.58	37.34	150.99	5.73
2	Cooling	15	4.42	64.26	230.11	8.82
3	Primary 45° WP Stream	6	10.96	111.0	566.06	21.69
4	Cooling	15	4.80	135.76	271.43	10.40
5	Dilution	6	14.22	192.13	952.88	36.51
6	Cooling	15	4.80	219.58	271.43	10.40

NOTE: Fuel Nozzle Area = 167.11 mm²
Percent Total Airflow = 6.40

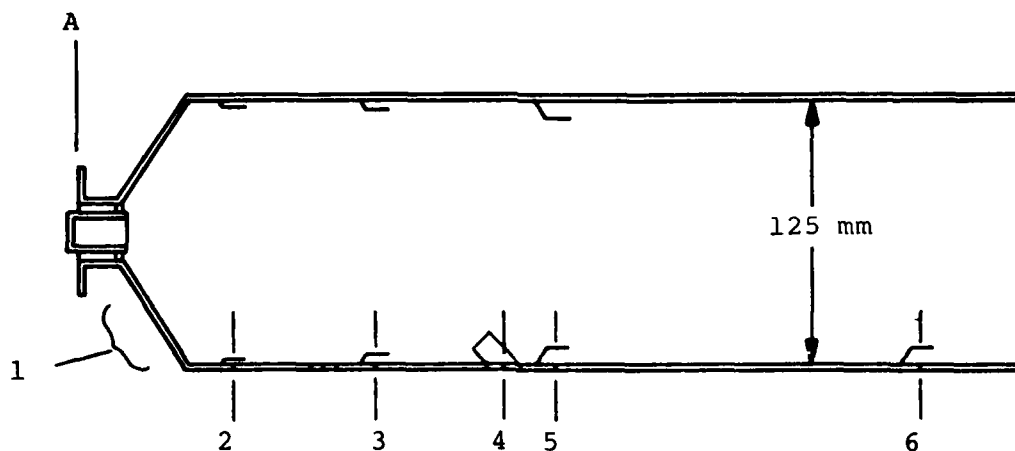
Figure 29. Mod IIA Combustor.



Row No.	Type Orifice	No. of Orifices	Orifice Diameter mm	Distance from A mm	Total Area mm ²	Airflow Percent Total
1	Cooling	15	3.58	37.34	150.99	6.52
2	Cooling	15	4.42	64.26	230.11	9.93
3	Primary 45° Up Stream	6	7.62	111.0	273.62	11.81
4	Cooling	15	4.80	135.76	271.43	11.71
5	Dilution	6	14.22	192.13	952.88	41.12
6	Cooling	15	4.80	219.58	271.43	11.71

NOTE: Fuel Nozzle Area = 167.11 mm²
Percent Total Airflow = 7.21

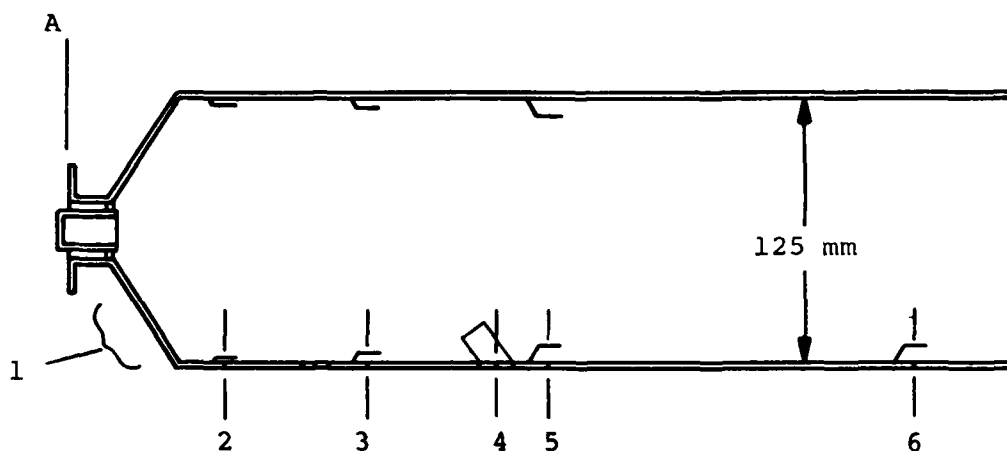
Figure 30. Mod IIB Combustor.



Row No.	Type Orifice	No. of Orifices	Orifice Diameter mm	Distance from A mm	Total Area mm ²	Airflow Percent Total
1	Cooling	15	3.58	37.34	150.99	4.48
2	Cooling	15	4.42	64.26	230.11	6.83
3	Cooling	15	4.80	135.76	271.43	8.06
4	Primary 45° Up Stream	6	10.96	192.13	566.06	16.81
5	Cooling	15	4.80	219.58	271.43	8.06
6	Dilution	6	19.05	322.40	1710.14	50.79

NOTE: Fuel Nozzle Area = 167.11 mm²
Percent Total Airflow = 4.96

Figure 31. Mod IIIA Combustor with Increased Primary Zone Residence Time.



Row No.	Type Orifice	No. of Orifices	Orifice Diameter mm	Distance from A mm	Total Area mm ²	Airflow Percent Total
1	Cooling	15	3.58	37.34	150.99	4.91
2	Cooling	15	4.42	64.26	230.11	7.48
3	Cooling	15	4.80	135.76	271.43	8.83
4	Primary 45° Up Stream	6	7.62	192.13	273.62	8.90
5	Cooling	15	4.80	271.43	271.43	8.83
6	Dilution	6	19.05	322.40	1710.14	55.62

NOTE: Fuel Nozzle Area = 167.11 mm²
Percent Total Airflow = 5.43

Figure 32. Mod IIIB Combustor.

of 0.0725, there did not appear to be any difference between flames produced by JP-4 and carbon slurry. The objective of the atmospheric rig testing was, therefore, achieved. Carbon-slurry fuel was burned with acceptable or negligible exhaust smoke levels within a reasonable length.

The last test on the atmospheric test rig was run with the Mod IIIB with the dilution orifices installed. The objective was to demonstrate complete combustion with minimal smoke. The test indicated that the flame was now contained within the combustor can, and there was no discernable difference between JP-4 and carbon-slurry flames. This concluded atmospheric rig testing and the flame visualization phase of the test program. Figure 33 shows the atmospheric rig operating on carbon slurry fuel. The information gained from this testing was then factored into the next series of testing, pressure-rig combustion evaluation on the ETJ131 combustion system. Also, fuel combustibility and handling information was transmitted to Suntech throughout the testing for formulation updating.

c. ETJ131 Combustor Pressure Rig Testing

The fuel that was selected for all of the pressure-rig testing and subsequent engine testing was approximately a 50-percent carbon, 50-percent JP-10 by weight mixture with a lead catalyst. The Suntech reference sample number for these samples was 790-974. The net heating value was approximately 167,500 BTU per gallon.

The ETJ131 combustor was modified to adjust the primary zone aerodynamics to accommodate the carbon-slurry fuel. The airflow distribution is shown in Figure 34. The initial test configuration included a standard vaporizer (ETJ131 hardware). The combustion system was installed in the combustor pressure-test facility with a one-gallon bladder delivery system for the carbon-slurry fuel. A baseline test was run on JP-4, and the hardware was inspected following the run to observe any distress.

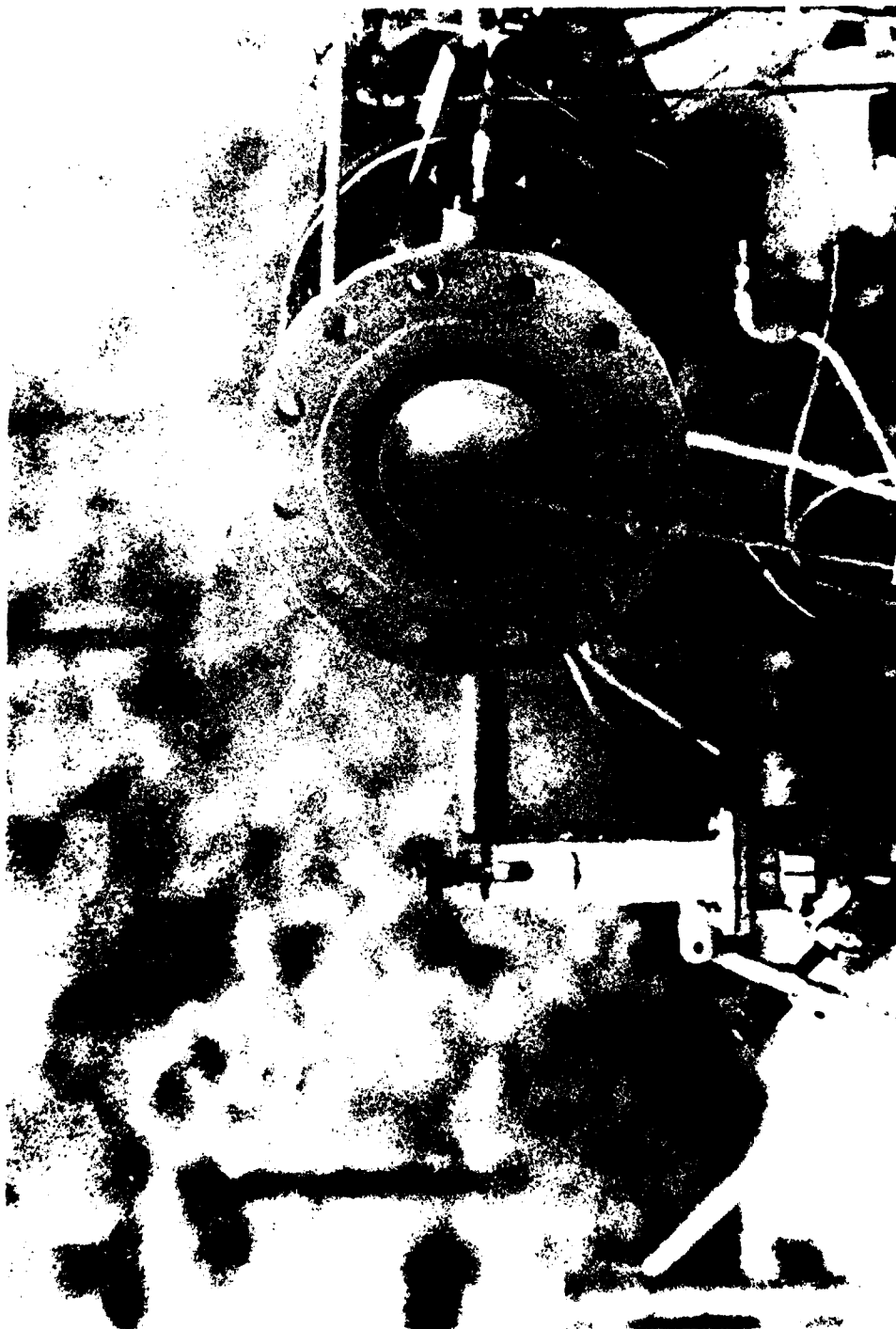
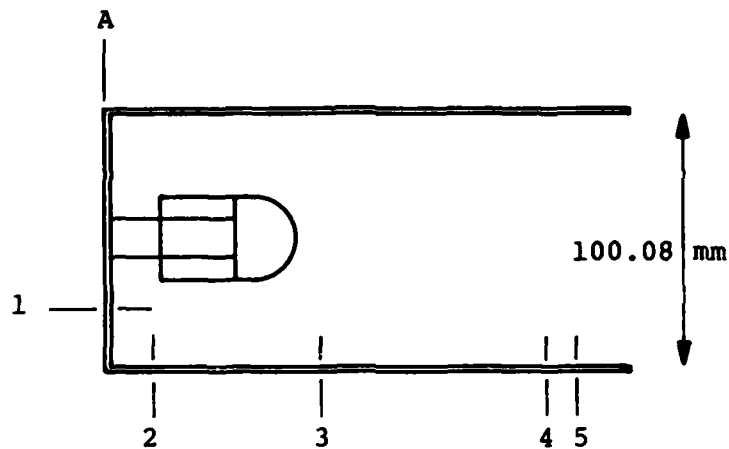


Figure 33. Atmospheric Combustor Operating on Carbon-Slurry Fuel.



Row No.	Type Orifice	No. of Orifices	Orifice Diameter mm	Distance from A mm	Total Area mm ²	Airflow Percent Total
1		10	6.35	0.	316.69	4.65
2		10	6.35	17.65	316.69	4.65
3	Primary	8	12.7	83.82	1013.31	14.88
4	Dilution	10	15.87	157.80	1978.08	29.05
5	Dilution	10	15.87	182.44	1978.08	29.05

NOTE: Mushroom Vaporizer Area = 1205.95 mm²
Percent Total Airflow = 17.71

Figure 34. Baseline ETJ131 Combustor.

All hardware was in satisfactory condition, so it was decided to proceed with a carbon-slurry run. The combustion system was ignited on JP-4 and stabilized at the maximum-power condition. The fuel delivery was then transitioned to carbon slurry and data recorded. The combustor ran for approximately 3 minutes on the carbon slurry (the time needed for consuming one gallon of fuel). The emissions and efficiency data from the test compared to JP-4 data are shown in Table 9. The efficiency variation for carbon-slurry fuel was due to the variability introduced into the efficiency calculation by unburned carbon from emissions. A 96-percent combustion efficiency was obtained based upon gaseous sample only.

TABLE 9. INITIAL PRESSURE-RIG TEST DATA WITH A VAPORIZING NOZZLE.

	JP-4	Carbon Slurry
Comb. Efficiency (%)	99.7	75-96
HC (gm/kg fuel)	0.563	1.475
CO (gm/kg fuel)	64.944	137.784
NO (gm/kg fuel)	3.735	5.534

General operation assessments for the initial run on carbon slurry at pressure conditions were satisfactory. Combustion stability appeared to be acceptable. No smoke data was recorded, but it was observed that smoke was considerably higher for carbon slurry than with JP-4. Upon teardown, the combustor was free of carbon, but the vaporizer was burned through. It was theorized that the mixture was near stoichiometric in the vicinity of the vaporizer where JP-10 was reacting. This resulted in excessive heating of the vaporizer. It was decided that the next modification was to incorporate primary-zone aerodynamic changes to

enrich the zone near the fuel nozzle. In addition, an airblast fuel nozzle similar to that used in atmospheric rig testing was installed in place of the vaporizer while fabricating a new vaporizer for subsequent tests.

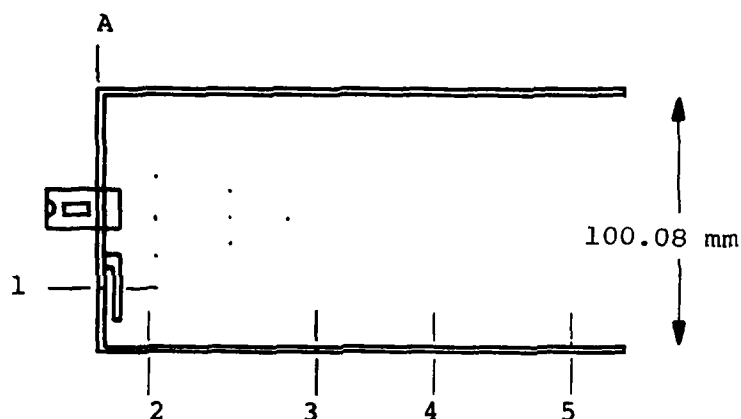
The second test was conducted with the modified ETJ131 combustor (Mod I) and an airblast nozzle as shown in Figure 35. The test procedure was the same as the first test. The test data is shown in Table 10.

TABLE 10. SECOND PRESSURE-RIG TEST DATA
WITH AIRBLAST NOZZLE.

	JP-4	Carbon Slurry
Comb. Efficiency (%)	99.8	75-96
HC (gm/kg fuel)	0.662	3.493
CO (gm/kg fuel)	30.559	124.460
NO (gm/kg fuel)	4.678	4.182

Combustion was not as stable during this run, as blowout occurred twice on carbon slurry. Upon teardown, no carbon was noted in the combustor liner, but a heavy buildup was noted in the passages of the airblast nozzle.

The Mod I combustor was also run with a modified vaporizer design to alleviate the vaporizer burning problem. This combustion system had emission performance comparable to the baseline combustor and also showed a less severe vaporizer burning problem. In view of the vaporizer structural durability problem, the combustor was modified to make it more compatible with the airblast nozzle and provide stable combustion. A six-inch combustor length was added to the intermediate combustion region to



Row No.	Type Orifice	No. of Orifices	Orifice Diameter mm	Distance from A mm	Total Area mm ²	Airflow Percent Total
1	Cooling	10	6.35	0.0	316.69	5.49
2		10	6.35	17.65	316.69	5.49
3	Primary	8	12.7	83.82	1013.31	17.56
4	Intermediate	10	15.87	130.8	1978.08	34.28
5	Dilution	10	15.87	182.44	1978.08	34.28

NOTE: Air Blast Atomizer = 167.11 mm²
 Percent Total Airflow = 2.90

Figure 35. Mod I Combustor with Low-Cost Airblast Atomizer.

provide more residence time to maximize carbon burnout. This modification was necessary because the ETJ131 combustor envelope resulted in a highly loaded combustor, as evident from the following computed combustor parameters:

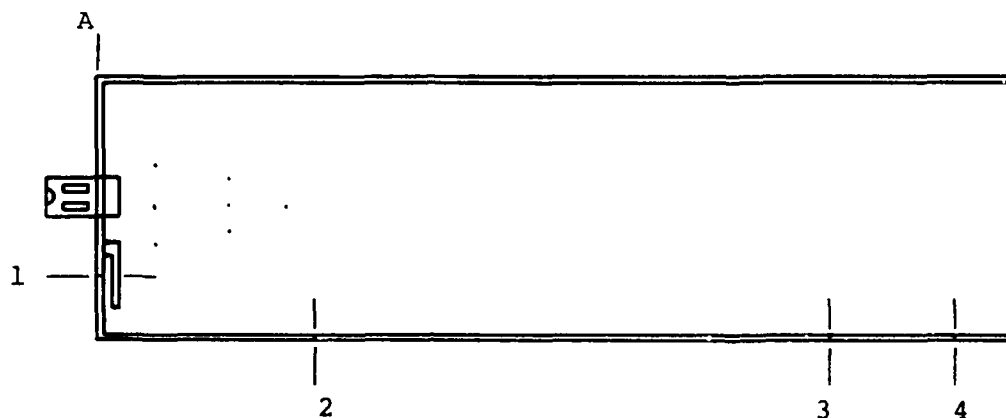
Heat Release Rate = $2310 \text{ J/S m}^3 \text{ Pa}$
 Loading Parameter = 18.26 kg/S m^3
 Reference Velocity = 61 m/S
 Burner Residence Time = 3 ms

The modified combustor, as shown in Figure 36, was tested both in the rig and the engine. During these tests, a known volumetric quantity of exhaust was passed through a filter for deposit smoke measurements. The filter was weighed before and after the smoke testing, thus giving the weight of carbon particles per unit volume of the exhaust. The measured emissions are presented in Table 11 for both JP-4 and the carbon-slurry fuel.

TABLE 3-11. THIRD PRESSURE-RIG TEST DATA OF MOD II COMBUSTOR WITH AIRBLAST NOZZLE.

	JP-4	Carbon Slurry
Gaseous Combustion Efficiency	99.84	--
Percent Carbon Burned	--	84
HC (gm/kg fuel)	0.17	--
CO (gm/kg fuel)	38.3	--
NO (gm/kg fuel)	7.39	--

Previous rig testing had shown that both JP-4 and the carbon-slurry fuels gave approximately the same levels of gaseous emissions. Therefore, in order to conserve on the limited quantity of the carbon-slurry sample, only smoke emission data was taken during the carbon-slurry test. The data showed that at the design point, 84 percent of the carbon in the carbon slurry could



Row No.	Type Orifice	No. of Orifices	Orifice Diameter mm	Distance from A mm	Total Area mm ²	Airflow Percent Total
1	Cooling	10	6.35	0.0	316.69	5.81
2	Primary	8	12.7	83.82	1013.31	18.58
3	Intermediate	10	15.87	289.56	1978.08	36.27
4	Dilution	10	15.87	341.12	1978.08	36.27

NOTE: Air Blast Atomizer = 167.11 mm²
Percent Total Airflow = 3.06

Figure 36. Mod II Combustor with Low-Cost Airblast Atomizer.

AD-A089 451

AIRESEARCH MFG CO OF ARIZONA PHOENIX F/G 21/4
COMPOUND CYCLE TURBOFAN ENGINE (CCTE). TASK IX. CARBON-SLURRY F--ETC(U)
MAR 80 T W BRUCE, H MONGIA F33657-77-C-0391
21-3365-A ML

UNCLASSIFIED

AFWAL-TR-80-2035

2 of 2

AD-A089 451



END
ONLY
FILMED
10-80
DTIC

be burned, indicating a need for further combustor development both in regard to residence time and combustor airflow distribution with attendant internal flow-field variations. However, further rig testing was considered beyond the scope of the present program. In summarizing the ETJ131 combustor rig testing, it was demonstrated that carbon-slurry fuels can be burned at the following flow conditions:

$$\begin{array}{ll} T_3 = 516K & P_3 = 3.79 \text{ kPa} \\ T_4 = 1227K & W_{a_3} = 1.18 \text{ kg/S} \end{array}$$

Whereas a 99.8-percent combustion efficiency was achieved with the JP-4, carbon slurry gave a combustion efficiency of 92-percent. Further improvement in combustion efficiency is considered feasible by modifying the combustion system and/or increasing the burner residence time. The combustion system (including fuel nozzle, combustor liner, and transition liner) did not show any discernable carbon fouling tendency. There are a number of development problems, including fuel delivery, ignition/restart, etc., that must be resolved to fully demonstrate feasibility of burning carbon-slurry fuel in a cruise-missile combustion system. However, all of these are deemed to be achievable within normal combustor development, assuming that reasonable fuel rheological properties can be maintained.

d. ETJ131 Demonstrator Engine Testing

The combustor configuration with airblast fuel nozzle resulting from the final pressure rig test was installed in the ETJ131 engine. The engine installed in the test facility is shown in Figure 37. A schematic of this engine with a dump combustor afterburner is shown in Figure 38. For testing in this program, the afterburner was not installed. The engine basically utilizes a turbocharger for the compressor and turbine components. It has a single-can combustor that provides an energy

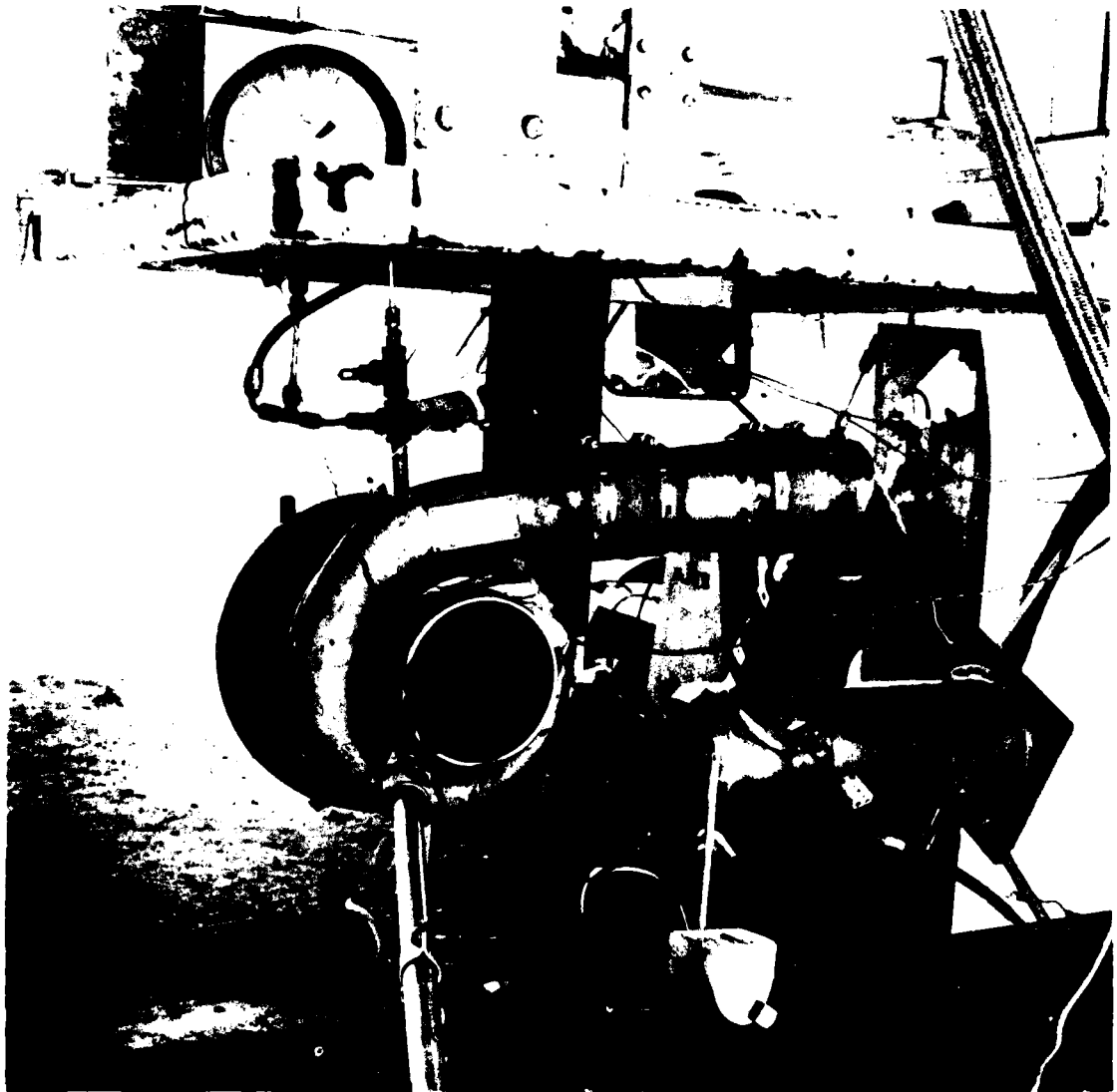


Figure 37. ETJ131 Engine Installed in Test Facility.

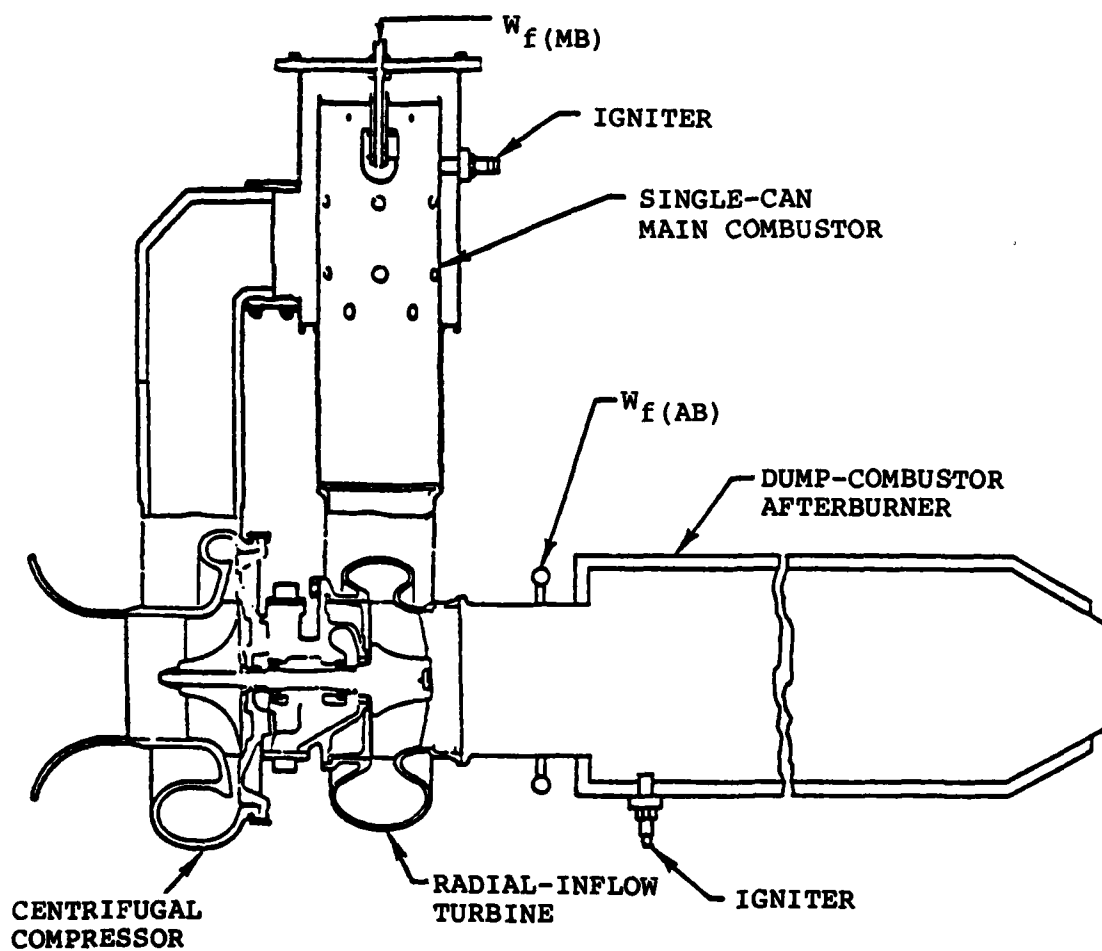


Figure 38. AiResearch Model ETJ131 Afterburning Turbojet Demonstrator Engine.

source and thus makes it an engine. This engine provided a desirable vehicle for the fuel demonstration testing because of its simplicity, ease of modification and low fuel consumption, which maximized available run time with limited fuel quantities. The carbon-slurry fuel used throughout was the same formulation as was used in the pressure-rig testing. The test procedure was to ignite and stabilize at maximum power on JP-4 before transitioning to carbon-slurry fuel from a bladder delivery system. The nature of the engine tests was for demonstration purposes only, and limited instrumentation was installed for obtaining quantitative data.

Two engine tests were conducted. The first was a five-minute run (total slurry run time) to check out the engine operation and inspect the hardware for any possible distress. The engine transitioned from JP-4 to carbon slurry at the maximum power condition with no indicated problem with stability. The engine operated satisfactorily on the carbon slurry, although more smoke was evident than with JP-4, presumably due to the fact that the combustion efficiency was lower than for JP-4 (as evidenced during pressure rig testing). However, during hardware inspection following the test, no carbon buildup on the combustor liner, fuel nozzle, or turbine component surfaces was noted.

Following completion of the checkout test and subsequent hardware inspection, the second engine test was conducted. The startup and fuel switchover procedure was the same as for the checkout test. Approximately one-half hour was accumulated on carbon slurry at the maximum-power condition. Fuel transition and combustion stability on the slurry were stable, and no problems or excessive temperatures were noted for the duration of the test. It appears that the combustion efficiency on the engine was somewhat lower than the rig, because a slightly higher fuel flow was required for the engine to attain equivalent exit temperature levels. As with the case with the rig, it is expected

that the combustion efficiency could be raised to an acceptable level through normal development. Again, smoke levels were greater for the carbon slurry than the JP-4, but this could be attributed to the combustion efficiency. No distress was noted on any of the combustor nozzle or turbine components.

The general assessments concluded from the combustion evaluation were encouraging. The slurries that were tested had rheological properties which were acceptable to fairly conventional means of pumping and atomization. As expected, the stability aspects of the fuel, which were not intended to be optimized for the delivered samples of this program, will need extensive development to obtain a high shelf life for the fuel. Ignition on carbon slurry will definitely be a challenge, especially for large passage airblast nozzles which will have low shearing capability at starting conditions because of low ΔP at that condition. The most important knowledge gained from the testing is the staged burning nature of the fuel wherein the JP-10 carrier is burned early followed by a much later reaction of the carbon. Therefore, future development will be required to optimize the combustor aerodynamics to accommodate this staged burning phenomena. Development will also be required to prevent the heavy carbon particles from being impinged on the combustor wall surfaces. It is believed that by successfully addressing these design criteria that a combustion system which can handle a carbon slurry fuel and extract the maximum amount of available energy within practical hardware constraints can be achieved.